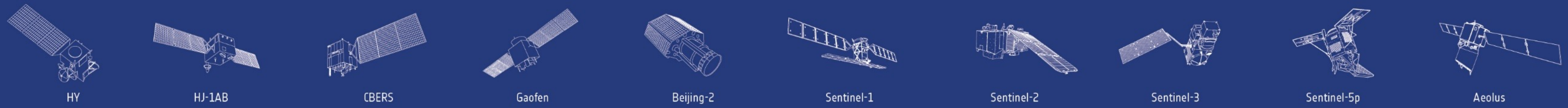

2023 DRAGON 5 SYMPOSIUM

3rd YEAR RESULTS REPORTING

11-15 SEPTEMBER 2023

PROJECT ID. 57160

MONITORING WATER PRODUCTIVITY IN CROP PRODUCTION AREAS FROM FOOD SECURITY PERSPECTIVES

13 SEPTEMBER 2023

ID. 57160

PROJECT TITLE: MONITORING WATER PRODUCTIVITY IN CROP PRODUCTION AREAS FROM FOOD SECURITY PERSPECTIVES

PRINCIPAL INVESTIGATORS: ZHU LIANG， DONG QINGHAN

CO-AUTHORS: WU BING FANG, MA ZONGHAN

PRESENTED BY: ZHU LIANG

Objectives

- Assess both the agricultural output and the water consumption for crop growth using satellite information and compute subsequently the water productivity
- The outcome of the research could be used as a scientific evidence for water use policy making

EO Data Delivery

Data access (list all missions and issues if any). NB. in the tables please insert cumulative figures (since July 2020) for no. of scenes of high bit rate data (e.g. S1 100 scenes). If data delivery is low bit rate by ftp, insert "ftp"

ESA Third Party Missions	No. Scenes
1.GeoEye-1/WorldView2	2
2.	
3.	
4.	
5.	
6.	
Total:	2

ESA, Explorers & Sentinels data	No. Scenes
1.Sentinel 2	16
2. MODIS	
3.	
4.	
5.	
6.	
Total:	16

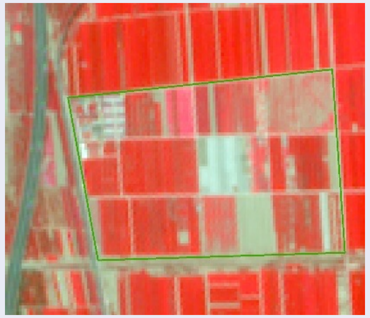

Chinese EO data	No. Scenes
1.GF-1, GF-2	4
2. FY	
3.	
4.	
5.	
6.	
Total:	4

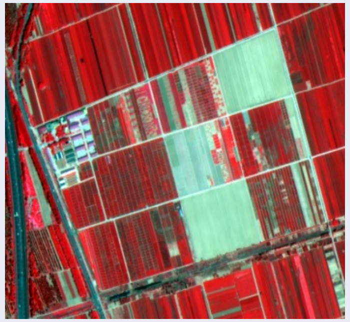

Schedule

- the project's schedule, planning & contribution of the partners

Monitoring water productivity in crop production areas from food security perspectives

Select a period to highlight at right. A legend describing the charting follows.

Period Highlight: | Plan Duration | Actual Start | % Complete | Actual (beyond plan) | % Complete (beyond plan)

	ACTIVITY	PLAN START	PLAN DURATION	ACTUAL START	ACTUAL DURATION	PERCENT COMPLETE
WP100	Field data collection					
	Field data collection and pre-processing of remote sensing and meteorological data - Season 1 + Season 2	1	24	1	24	100%
	TerraScope Training	9	2	9	2	100%
WP200	Crop type identification					
	Crop type mapping for the study regions - Season 1 + 2	9	16	9	16	100%
	Validation or comparison with the local official statistics - Season 1+2	26	2	26	2	100%
MS1	Milestone 1 (MS1) – 1 ESA Dragon 5 Conference report	12	1	12	1	100%
WP300	Crop Yield forecasting					
	Crop yield modeling for the study regions - Season 1 + 2	13	12	13	12	100%
	Validation or comparison with the local official statistics - Season 1 + 2	25	2	25	2	100%
MS1	Milestone 2 (MS2) – 1 conference report / 1 peer-reviewed Journal article	29	1	29	1	100%
WP400	Evapotranspiration and water productivity mapping (WPM)					
	Maps of actual ET per targeted crop – Season 1+2	27	3	27	3	100%
	Water productivity maps for each study region and for each crop - Season 1+2	30	3	30	3	100%
	Validation or comparison with the local official statistics - Season 1+2	33	2	33	2	100%
MS3	Milestone 3 (MS3) – 1 ESA Dragon 5 Conference report / 1 peer-reviewed Journal article	35	1	35	1	100%
FR	Final Report	36	1	36	1	100%

PERIODS: 1 2 3 4 5 6 7 8 9 10 11 12 13 14 15 16 17 18 19 20 21 22 23 24 25 26 27 28 29 30 31 32 33 34 35 36

ETWatch Model

Characterizing earth surface with multi-source remote sensing data

Quantifying fluxes between surface and atmospheric boundary layer

Integration of energy balance, aerodynamics and water balance

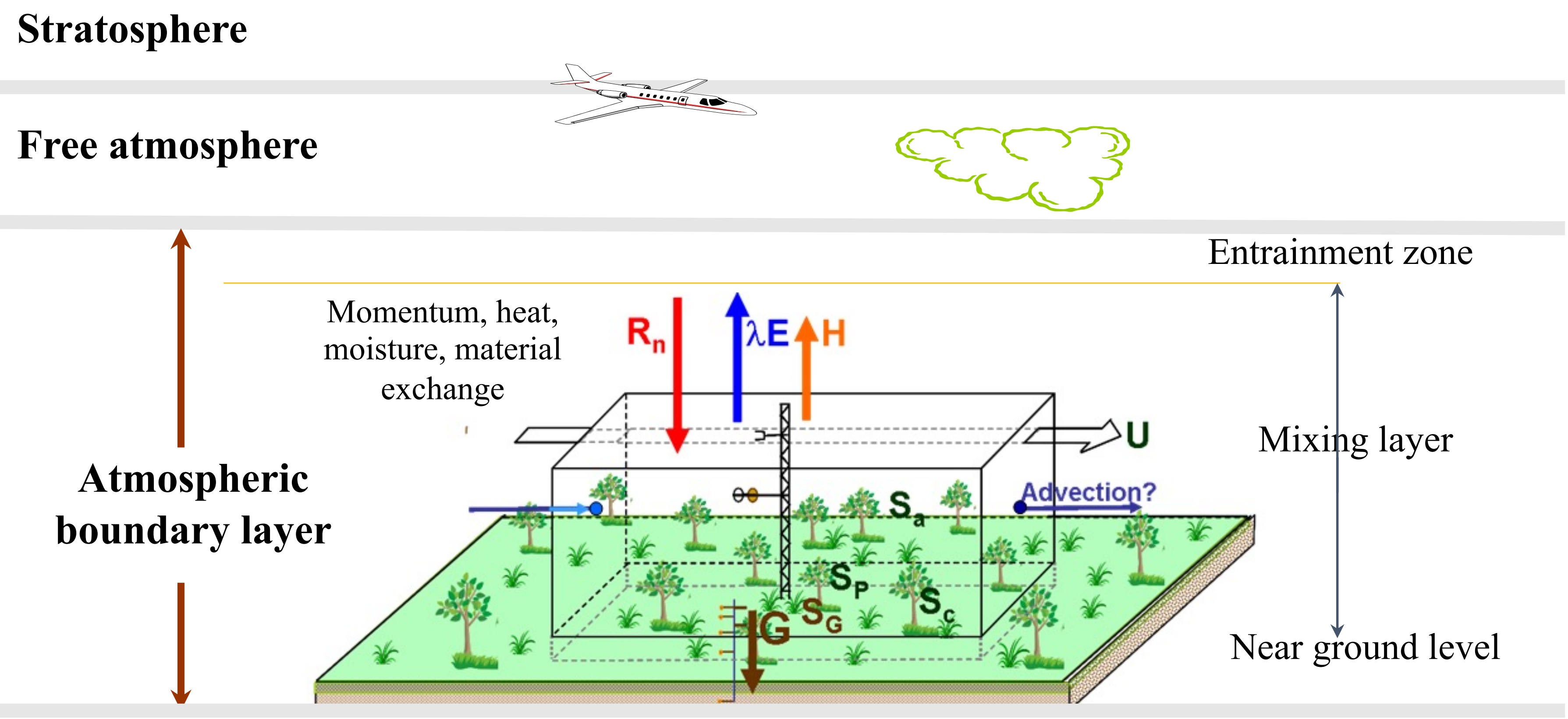

ETWatch–operational remote sensing model

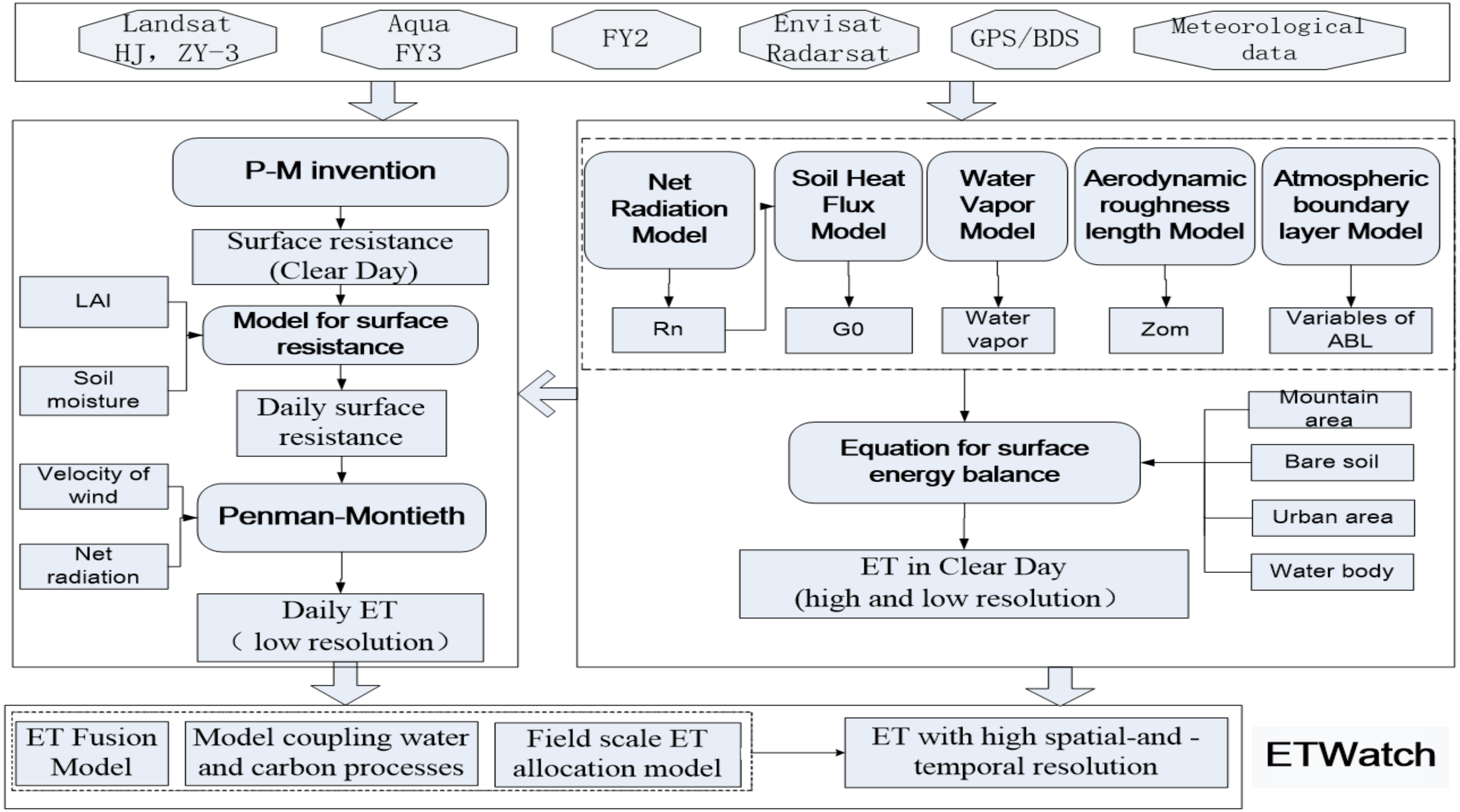

Sub-models

- *Parametrized*
  - Net-radiance model
  - Soil heat flux model
  - Sensible heat flux model
  - Latent heat flux model
- *key parameters model*
  - Aerodynamic roughness length model
  - Atmospheric Boundary Layer model
  - Vapor pressure deficit model
  - Canopy conductance model
- *ET scale conversion model*

➢ Net-radiance model
➢ Surface soil heat flux model
➢ Aerodynamic roughness length model
➢ Atmospheric Boundary Layer model
➢ Vapor pressure deficit model
➢ Canopy conductance model
➢ Sensible heat flux model
➢ Latent heat flux model
➢ Bare soil evaporation model
➢ Water surface evaporation model
➢ Ice snow sublimation model
➢ Latent heat flux model
➢ ET fusion model
➢ Coupling water and carbon processes Model
➢ Field scale ET allocation model

Input data

Parameter	Description	Data Source	Clear day	Cloud day
LST	Land surface temperature	**MODIS/FY3**	○	×
Albedo	Surface reflectivity of solar radiation	**MODIS/FY3/Sentinel-2**	○	○ With Filter method
LAI	Leaf Area Index	**MODIS/FY3/Sentinel-2**	○	○ With LAI-NDVI
Meteo parameters	Relative Humidity, Wind Velovity, Sun Shine Hours, Air Presure, Air Temperature	**Meteo**	○	○
PBL	Air temperature, Wind Velovity, Air Presure and Humidity of Boudary Layers	**ARIS**	○	○ With Filter method
VPD_es	Instantaneous near-surface saturated vapour pressure	**MODIS/FY3**	○	○ With gap filing
VPD_ea	Instantaneous near-surface actual vapour pressure	**MODIS/FY3**	○	○ With gap filing
Gc	Canopy Conductance	**MODIS/FY3**	○	○ With gap filing
Rnl	Net longwave radiation	**MODIS/FY3**+meteo	○	○ With gap filing

Challenges 1: Complex underlying surface

- ***Complex underlying surface within pixel of remote sensing does not match the homogeneous underlying surface which is assumed with ET model***
  - ✓ Parameter values for specific underlying surface types are not suitable for mixed pixels
  - ✓ Models with high uncertainty and poor regional applicability

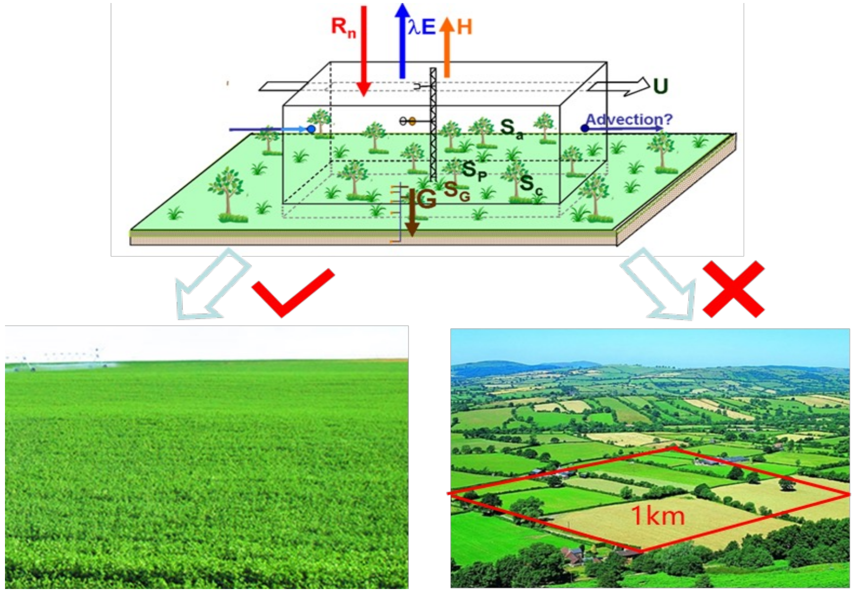

Ideal underlying surface

Actual underlying surface

Types	Maximum canopy height (m)	Minimum vegetation canopy resistance (m/s)	VPD sensitive parameter (1/hPa)
Forest land	20	100	0.025
Grassland	0.2	40	0.0155
Wetland	0.01	150	0.0155
Cultivated land	2	40	0.023
Bare land	0.05	50	-

Parametric values assumed by pure feature type are not suitable for mixed pixels

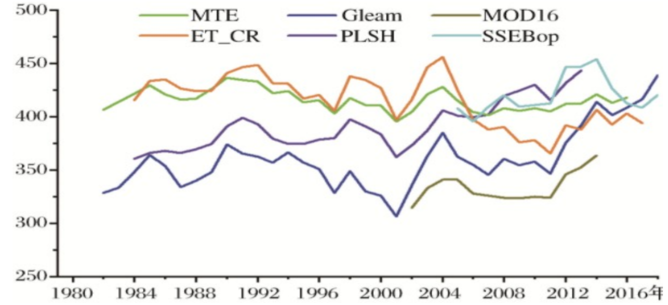

Model uncertainty and regional applicability

Daily surface soil heat flux

- ***Surface soil heat flux is the key to increasing the monthly energy closure rate, which seriously affects the accuracy of monthly and seasonal evapotranspiration (about 5-10%)***
  - Existing evapotranspiration models all assume that the daily surface soil heat flux is zero
  - Daily surface soil heat flux models is proposed based on the daily diurnal surface temperature
  - Improved monthly energy balance closure rate, monthly evapotranspiration accuracy can be increased by 3-5%

$$G(z,t) = D_h \frac{\partial}{\partial z} T(z,t) = D_h \frac{1}{\sqrt{D_h}} \frac{\partial^{(1/2)}}{\partial t^{(1/2)}} \left[T(z,t) \quad T_0 \right]$$

$$G(t) = \sqrt{\frac{D_h}{\pi}} \int_0^t \frac{dT(s)}{\sqrt{t \quad s}} = \frac{\Gamma}{\sqrt{\pi}} \int_0^t \frac{dT(s)}{\sqrt{t \quad s}}$$

$$\Gamma = f(\Delta T, \text{albedo}, S_0, \omega, \delta, C_r, \phi)$$

$$G_0(t) = G(0,t)$$

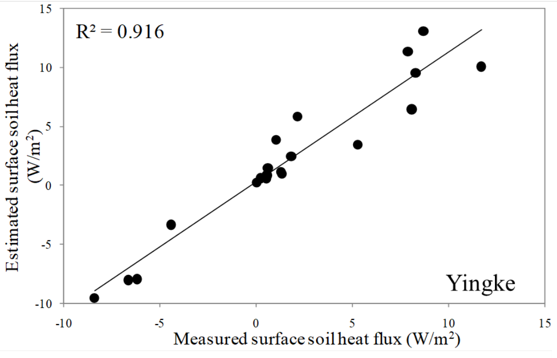

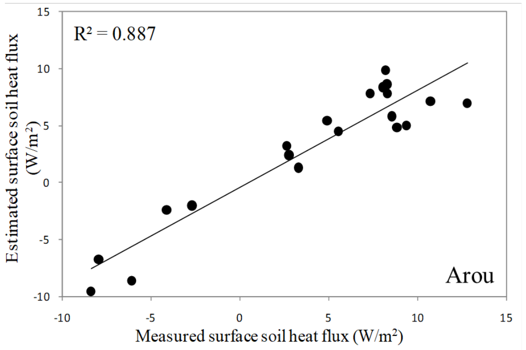

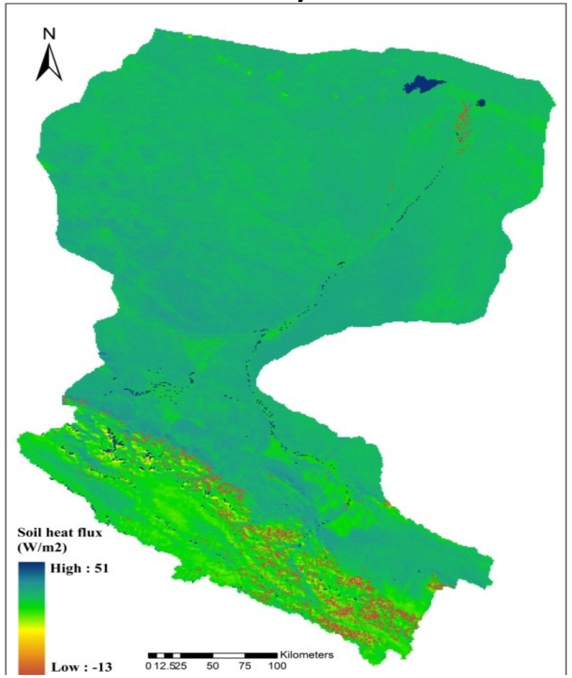

•*Zhu WW, Wu B F, et al. 2014. A method to estimate diurnal surface soil heat flux from MODIS data for a sparse vegetation and bare soil. Journal of Hydrology, 511, 139-150.*

Canopy stomatal conductance model

- ***Canopy stomatal conductance model is proposed, and the empirical value of the maximum stomatal conductance is replaced by a mathematical model to reflect the spatial heterogeneity of vegetation types and the influence of the atmospheric environment.***

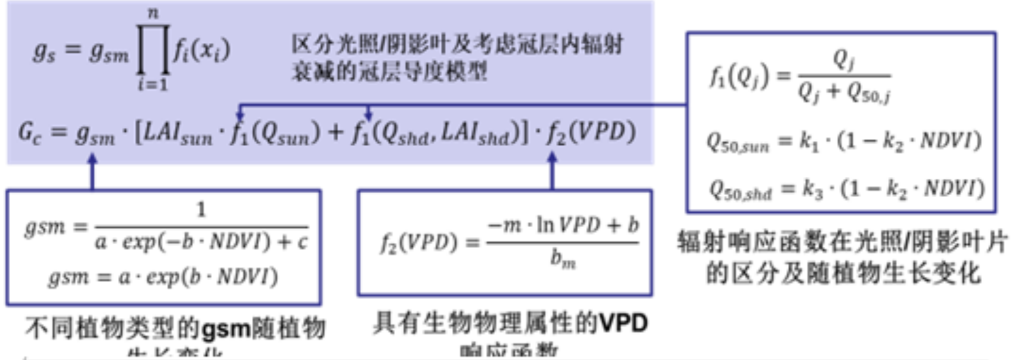

	Gs					ET				
Sites	Slope	Intercept (ms^{-1})	R^2	RMSE (ms^{-1})	Gsmeas (ms^{-1})	Slope	Intercept (mm)	R^2	RMSE (mm)	ETmeas (mm)
GT-W	0.91	0.0004	0.89	0.0023	0.0078	0.90	0.08	0.93	0.55	2.59
GT-M	0.76	0.0009	0.6	0.0025	0.0064	1.04	-0.39	0.92	0.47	3.01
HL	0.79	0.0006	0.77	0.0015	0.0033	0.89	0.15	0.91	0.47	1.78
MY	0.49	0.0034	0.47	0.0038	0.0065	0.89	0.61	0.82	1.05	2.85
AR	0.87	0.0013	0.89	0.0032	0.0092	0.96	0.05	0.99	0.2	1.62
Guantan	0.47	0.0017	0.63	0.002	0.0032	0.88	0.26	0.71	0.69	1.22
DM	0.81	0.0008	0.81	0.0022	0.0044	0.96	0.10	0.95	0.45	1.98
ZY	0.67	0.0014	0.65	0.0038	0.0083	0.96	-0.15	0.94	0.68	3.61
SDQ	0.93	0.001	0.65	0.0009	0.0018	1.03	0.25	0.9	0.7	1.70

Validation of the model: statistical metrices

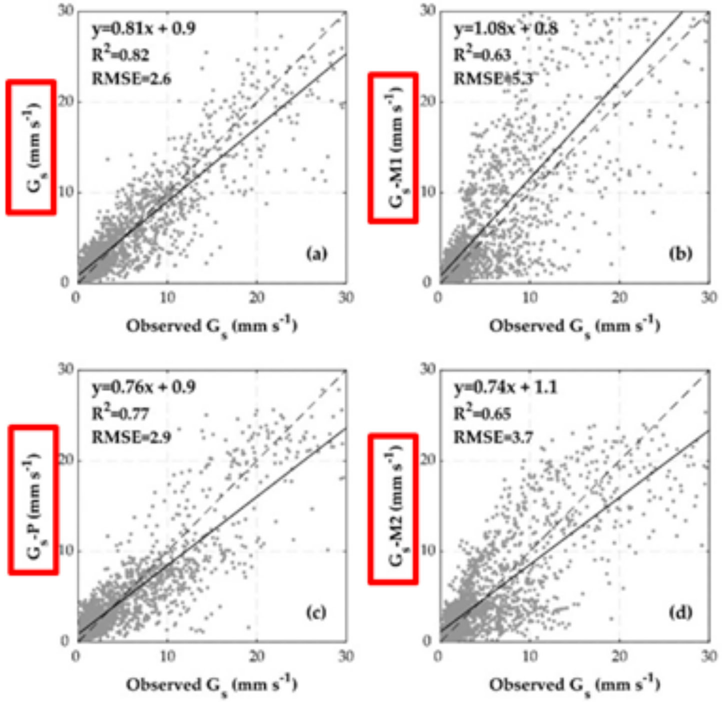

Gs: the model
Gs-M1, Gs-M2: other models
Gs-P: the model with reduced parameters

Xu J M, Wu B F, et al. 2021. A Canopy Conductance model with temporal physiological and environmental factors. STOTEN. 791, 148283

Xu J M, Wu B F, et al. 2020. Quantifying the contribution of biophysical and environ. factors in uncertainty of canopy conductance. Journal of Hydrology, 592:125612

Aerodynamic roughness length (ARL) models

- ***Aerodynamic roughness is a key variable that affects evapotranspiration. If the influence of topography, micro-topography and canopy structure is not considered, it is easy to cause large evapotranspiration errors on complex underlying surfaces such as non-growing seasons, mountainous areas, and urban areas.***

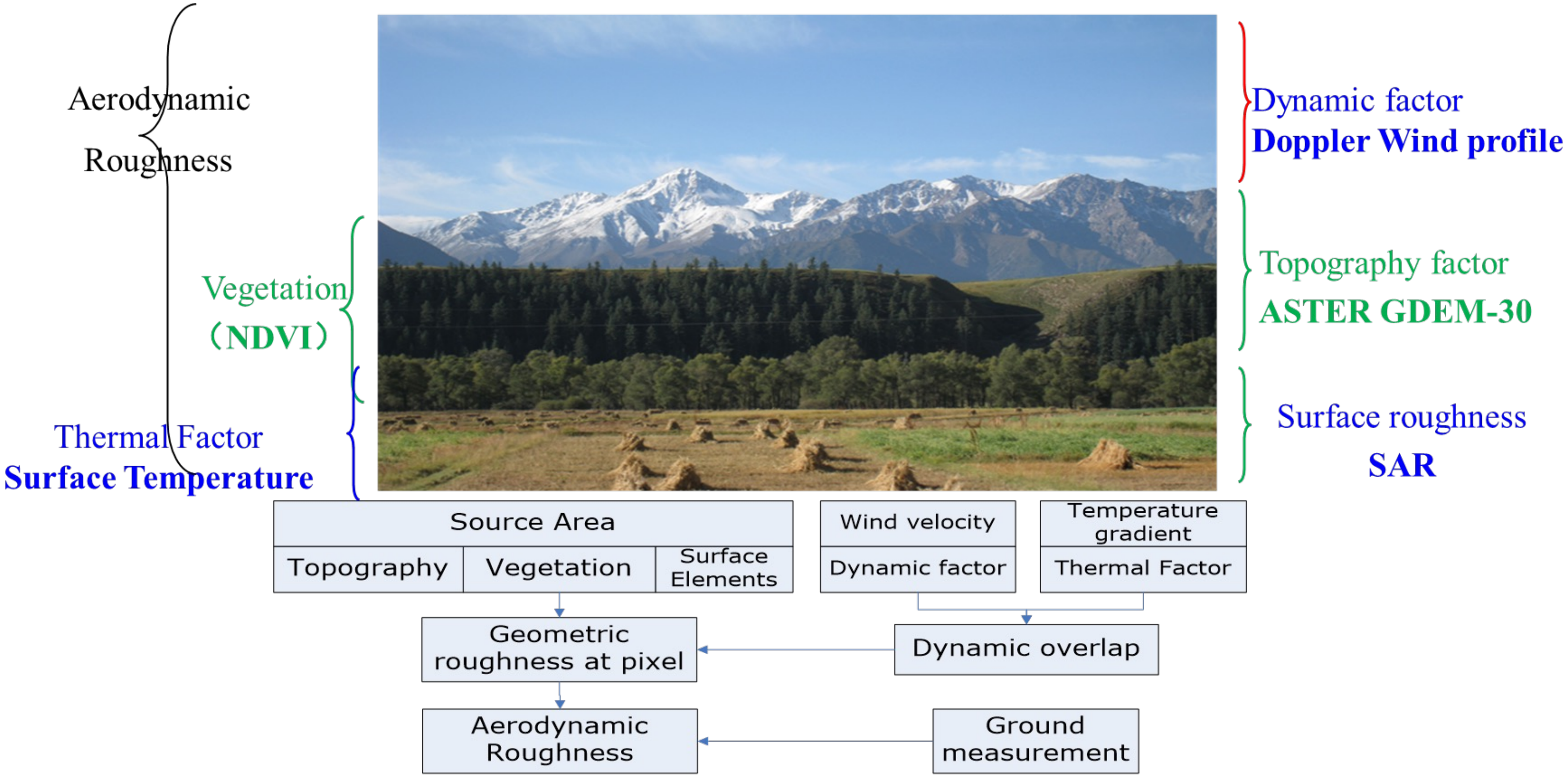

Vegetation structure for ARL with MODIS BRDF Parameter

BRDF Model: $\rho(\theta_s, \theta_v, \phi) = k_0 + k_1 F_1(\theta_s, \theta_v, \phi) + k_2 F_2(\theta_s, \theta_v, \phi)$

The bi-directional reflectance characteristics fitting based on RossThick and LiSparseR kernel

$$\mathrm{BRDF\_}R = k_2 / k_0$$

The factor R can reflect the heterogeneity of surface geometric structure

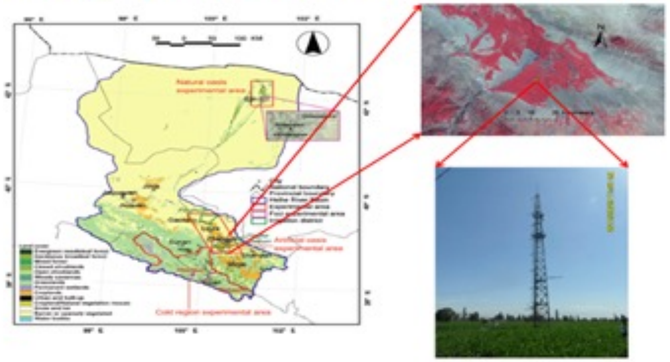

Daman in the middle reaches of Heihe River Basin

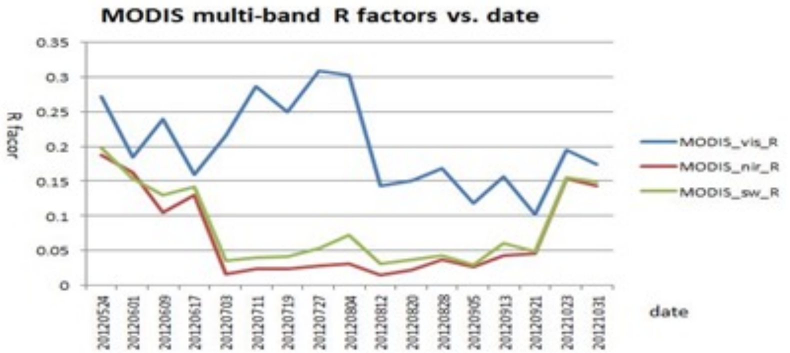

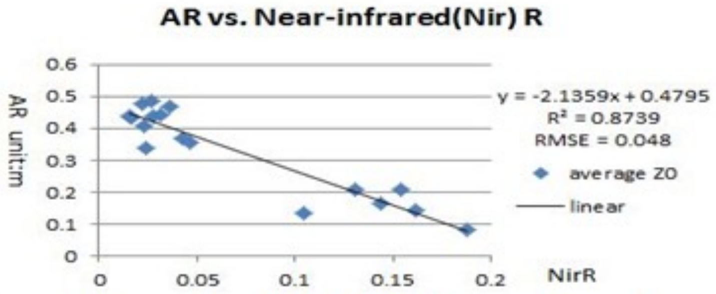

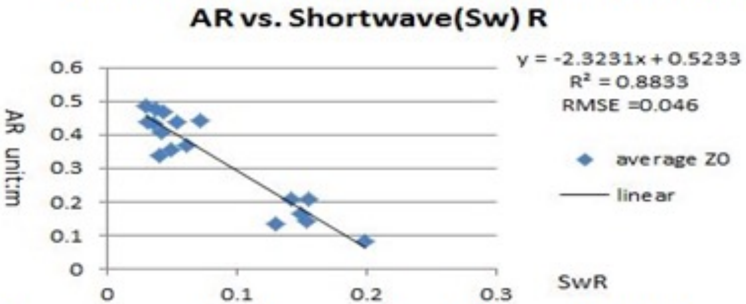

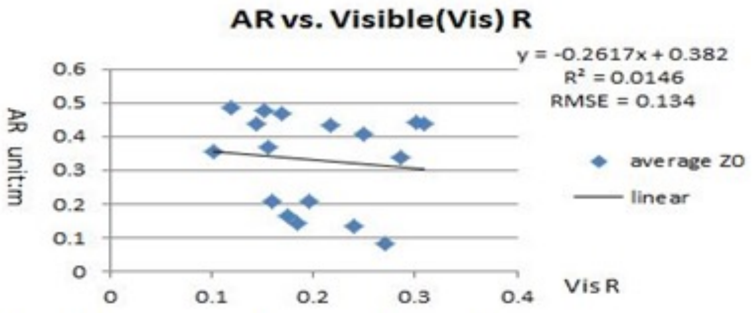

Conclusion: the BRDF information of near-infrared or shortwave band is suitable to estimate temporal aerodynamic roughness length over farmland with equivalent effect.

Wu Bingfang, Xing Qiang, Yan Nana, Zhu Weiwei, Zhuang Qifeng. A linear relationship between temporal multiband MODIS BRDF and aerodynamic roughness in HiWATER wind gradient data, IEEE Geoscience and Remote Sensing Letters, 2015, 12, 507–511.*

Topographic Roughness for ARL with DEM

- *Two dimensional RMSH Definition*
- *Input data: DEM*

$$\bar{z} = \frac{1}{LxLy}\int_{-Lx/2}^{Lx/2}\int_{-Ly/2}^{Ly/2} z(x,y)dxdy$$

$$\overline{z^2} = \frac{1}{LxLy}\int_{-Lx/2}^{Lx/2}\int_{-Ly/2}^{Ly/2} z^2(x,y)dxdy$$

$$RMSH = (\overline{z^2} - \bar{z}^2)^{1/2}$$

$\bar{z}$: Average of the image

$\overline{z^2}$: Two moment

RMSH: Root-mean-square height

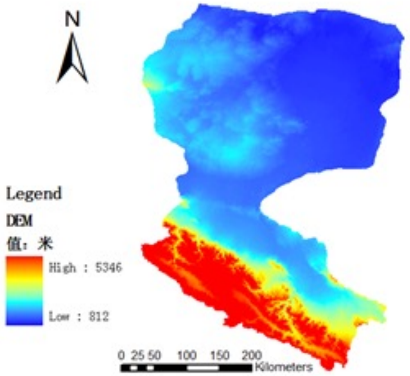

DEM with 1km resolution

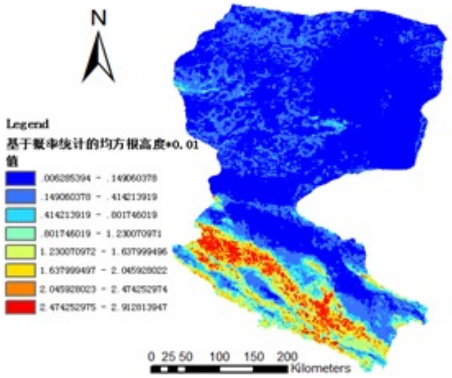

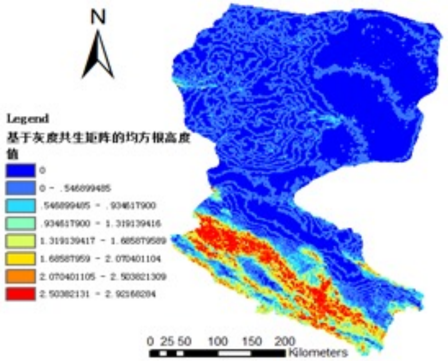

Wu Bingfang, Zhu Weiwei, Yan Nana, Xing Qiang, Xu Jiaming, Ma Zonghan, Wang Linjiang. Regional actual evapotranspiration estimation with land and meteorological variables derived from multi-source satellite data. Remote Sensing, 2020, 12, 332

Geometric roughness for ARL with backscattering

- *The geometric roughness keeps stable for one fixed land cover usually*
- ***Input data: radar backscattering data***

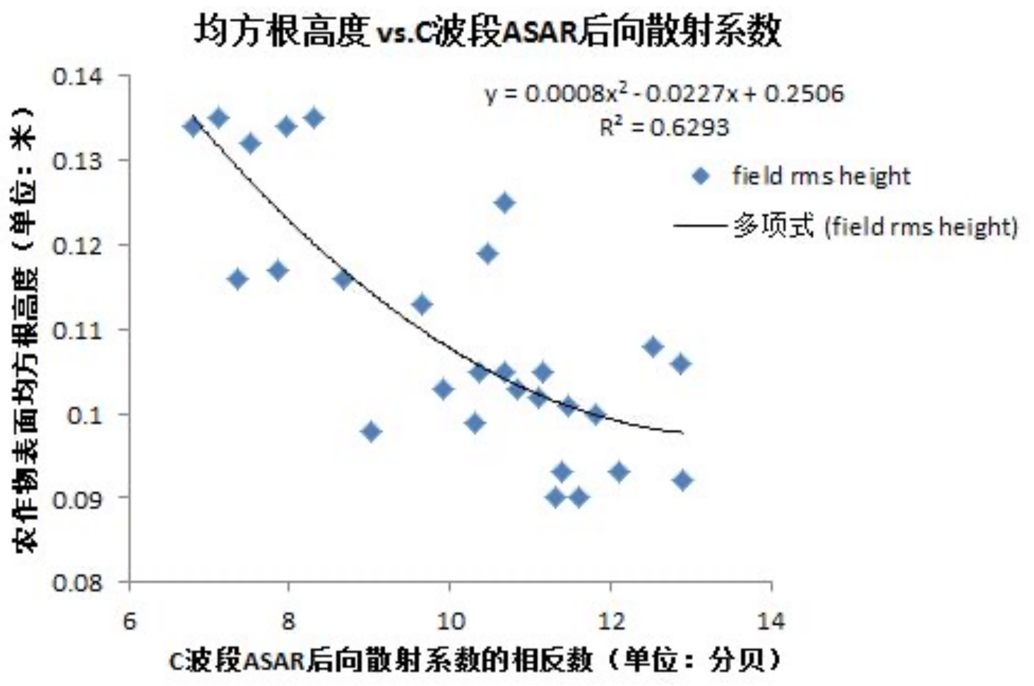

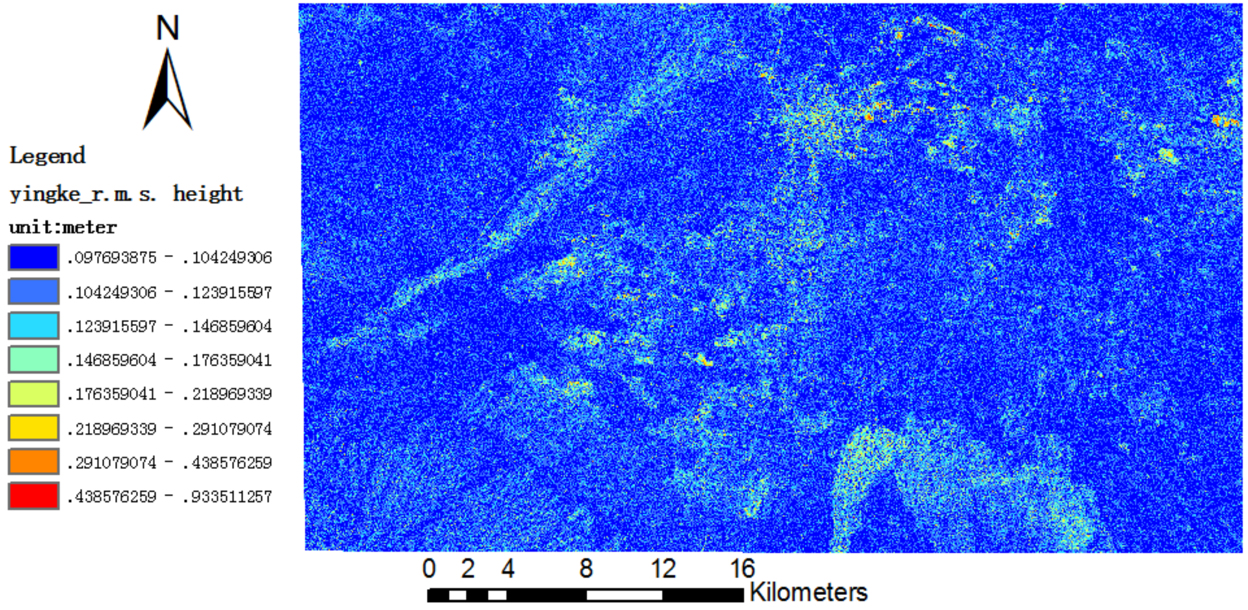

Inversed Geometric Roughness

Wu Bingfang, Zhu Weiwei, Yan Nana, Xing Qiang, Xu Jiaming, Ma Zonghan, Wang Linjiang. Regional actual evapotranspiration estimation with land and meteorological variables derived from multi-source satellite data. Remote Sensing, 2020, 12, 332

New ARL models for the complex underlying surface

- ***Coupled with multi-dimensional data such as optics, infrared, microwave, topography, etc., an aerodynamic roughness model is proposed, which reveals the daily change process of aerodynamic roughness, and significantly reduces the evapotranspiration error in non-growing seasons, mountainous areas, and urban areas, ensuring daily and Ten-day evapotranspiration error <7%.***

  - *The overall components of the composited aerodynamic Roughness*

    $$A_{zom} = (Z^{v}_{0m} + Z^{nir}_{0m}) \cdot (1 + (slope - a_1) > 0/a_2) + Z^{r}_{0m}$$

  - The vegetation component based on NDVI

    $$Z^{v}_{0m} = b_1 + b_2 \cdot ((NDVI) > 0/NDVI_{max})^{b_3}$$

  - The geometric structure based on near-infrared R factor

    $$Z^{nir}_{0m} = e^{c_1 \cdot \frac{f_{geo}}{f_{iso}} + c_2}$$

  - The hard surface roughness based on radar backscattering coefficient

    $$Z^{r}_{0m} = e^{d_1 \cdot sigma_0 + d_2}$$

Wu B F, et al. 2020. Regional actual evapotranspiration estimation with land and meteorological variables derived from multi-source satellite data. Remote Sens, 12(2), 332.
Wu B F, et al. 2015. A Linear Relationship between temporal multiband MODIS BRDF and aerodynamic roughness. IEEE GRSL, 12(3), 507-511.
Yu M Z, Wu B F, et al. 2016. A method for Estimating the Aerodynamic Roughness Length with NDVI and BRDF Signatures. Remote Sensing, 9(6), 2017

Validation of Aerodynamic roughness length

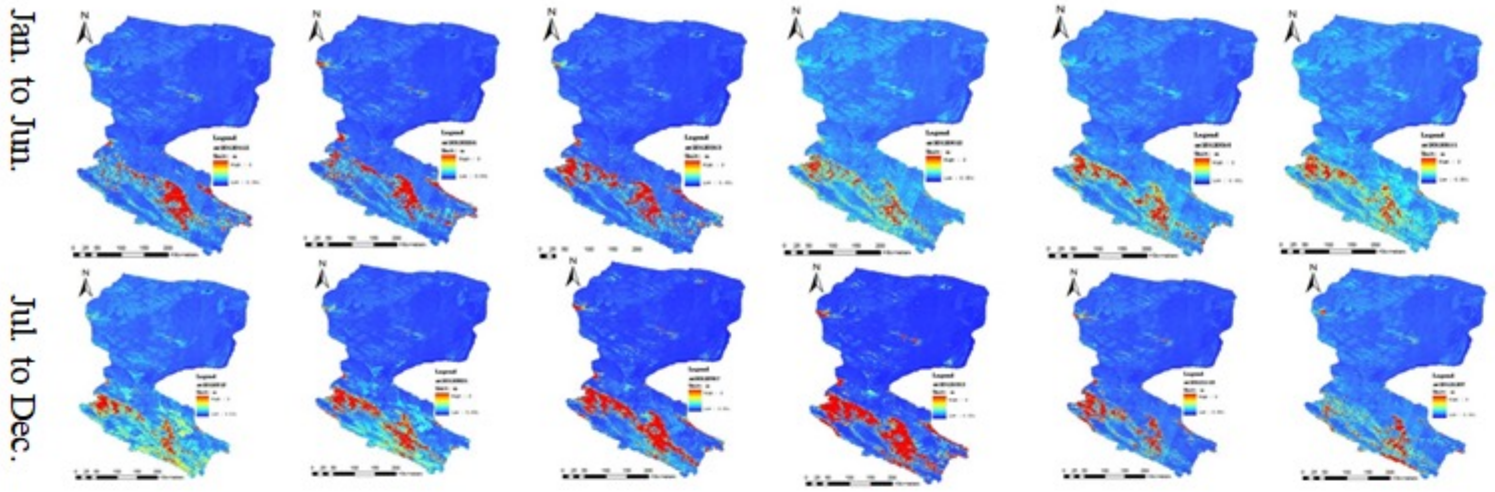

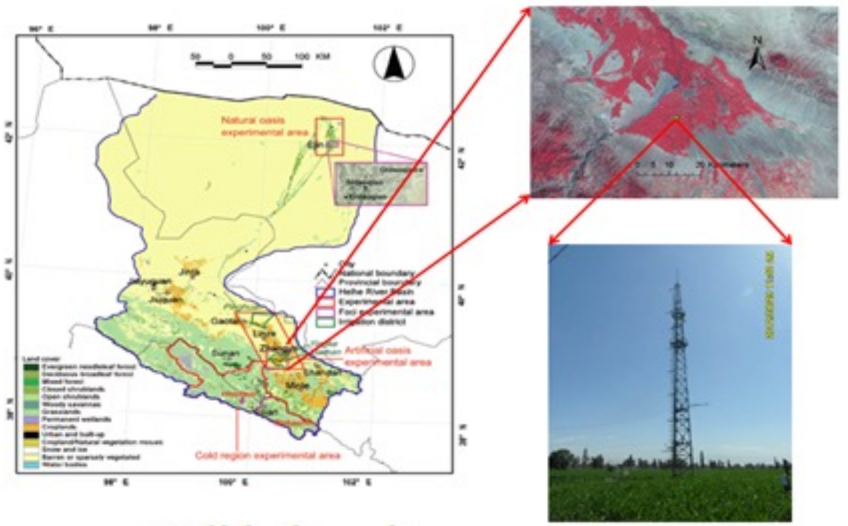

Change trend comparison between wind gradient and remote sensing based aerodynamic roughness

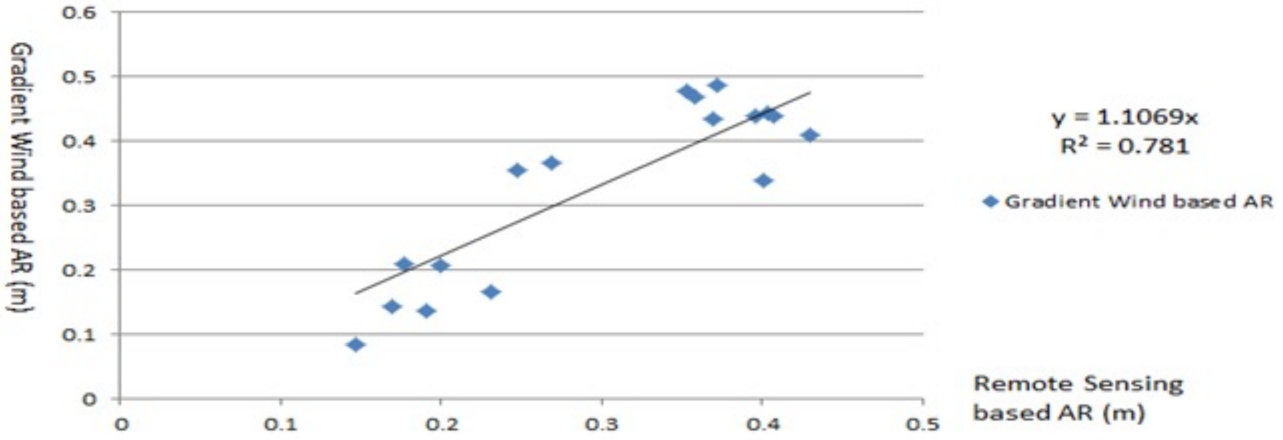

Scatter chart between wind gradient and remote sensing based aerodynamic roughness

Challenges 2: Multicollinearity problem

- ***Multicollinearity problem between key variables in ET models.*** The same VI is redundantly used to calculate several key variables in ET models.
  - ✓ NDVI was used to calculates net radiation, soil heat flux, roughness in the SEBAL model
  - ✓ LAI is used to calculate net radiation, soil heat flux, roughness, KB-1 in the SEBS model
- ***There is high correlation between key variables, leading to unstable parameter estimates, large systematic bias and inter-annual variability.***

SEBAL

$$R_n = (1-\alpha)R_{S\downarrow} - R_{L\uparrow} - (1-\varepsilon_0)R_{L\downarrow}$$

$$\varepsilon_0 = a + b\ln(\mathrm{NDVI})$$

$$G/R_n = T_S/\alpha(0.0038\alpha + 0.0074\alpha^2)(1-0.98NDVI^4)$$

$$z_{0m} = \exp(a \times NDVI + b)$$

$$r_{ah} = \frac{\ln\left(\frac{z_2}{z_1}\right) - \Psi_{h(z_2)}}{u_* \times k} \qquad \frac{u_x}{u_*} = \frac{\ln\left(\frac{z_x}{z_{0m}}\right)}{k}$$

$$H = \frac{\rho_{air} \times Cp_{air} \times dT}{r_{ah}}$$

$$\Lambda = \frac{R_n - G_0 - H}{R_n \quad G_0}$$

$$ET_{24} = \frac{86400\Lambda(R_{n24} - G_{024})}{\lambda}$$

SEBS

$$R_n = (1-\alpha)R_{S\downarrow} - R_{L\uparrow} - (1-\varepsilon_0)R_{L\downarrow}$$

$$\varepsilon_0 = a + b\ln(\mathrm{LAI})$$

$$LAI = \frac{\log(1-f_c)}{-\Lambda}$$

$$G = R_n[\Gamma_c + (1-f_c)(\Gamma_s - \Gamma_c)]$$

$$\theta_0 - \theta_a = \frac{H}{ku_*\rho C_p}\left[\ln\left(\frac{z-d_0}{z_{0h}}\right) - \Psi_h\left(\frac{z-d_0}{L}\right) + \Psi_h\left(\frac{z_{0h}}{L}\right)\right]$$

$$z_{0h} = z_{0m}/\exp(kB^{-1})$$

$$z_{0m} = 0.005 + 0.5\left(\frac{NDVI}{NDVI_{max}}\right)^{2.5}$$

$$kB^{-1} = \frac{kC_d}{4C_t\frac{u_*}{u(h)}(1-e^{-n_{ec}/2})}f_c^2 + 2f_c^2f_s^2\frac{ku_*/u(h)z_{0m}/h}{C_t^*} + kB_s^{-1}f_s^2$$

$$n_{ec} = \frac{C_d \cdot LAI}{2u_*^2/u(h)^2}$$

$$H_{wet} = R_n - G - \lambda E_{wet}$$

$$\lambda E_{wet} = R_n - G - H_{wet}$$

$$\Lambda_r = \frac{\lambda E}{\lambda E_{wet}} = 1 - \frac{\lambda E_{wet} - \lambda E}{\lambda E_{wet}} = 1 - \frac{H - H_{wet}}{H_{dry} - H_{wet}}$$

$$\Lambda = \frac{\lambda E}{R_n - G} = \frac{\Lambda_r \cdot \lambda E_{wet}}{R_n - G} = \Lambda_r\left(1 - \frac{H_{wet}}{H_{dry}}\right)$$

$$E_{daily} = \sum_{i=0}^{24}\left[\Lambda\frac{R_n - G}{\lambda\rho_w}\right] = 24 \times 3600 \times \left[\frac{\lambda E}{\lambda \cdot \rho_w}\right]$$

Key variables such as NDVI, LAI from a single sensor are reused many times in the existing remote sensing ET models

Daily net radiation model

- ***Clouds are a key factor affecting net radiation and it is difficult to accurately quantify surface solar radiation using MODIS /LandSat data***
  - Sunshine hours and net daily radiation models are proposed based on the hourly cloud data products of geostationary meteorological satellites
  - It solves the problem of accurately describing the changes in the temporal and spatial distribution of daily shortwave radiation, daily net longwave radiation, and daily net daily radiation, and also solves the problem of calculating daily net radiation on cloudy and rainy days.

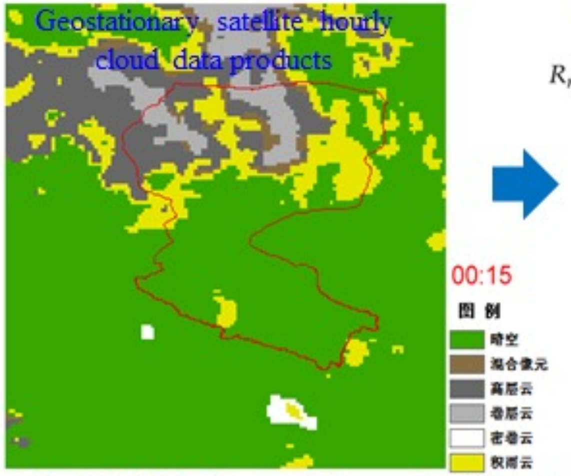

Daily net radiation model

$$R_{n,daily} = (1-\alpha)\cdot\left(a_s + b_s\frac{n}{N}\right)R_a - R_{nl}$$

$$n = \sum_{i=t_r+0.25}^{i=t_s-0.25} F_i * t_g$$

代码	云类型	日照因子
0/1	晴天	0.90
11	混合像元	0.21
12	高层云或雨层云	0.25
13	卷层云	0.51
14	密卷云	0.24
15	积雨云	0.13
21	层积云或高积云	0.35

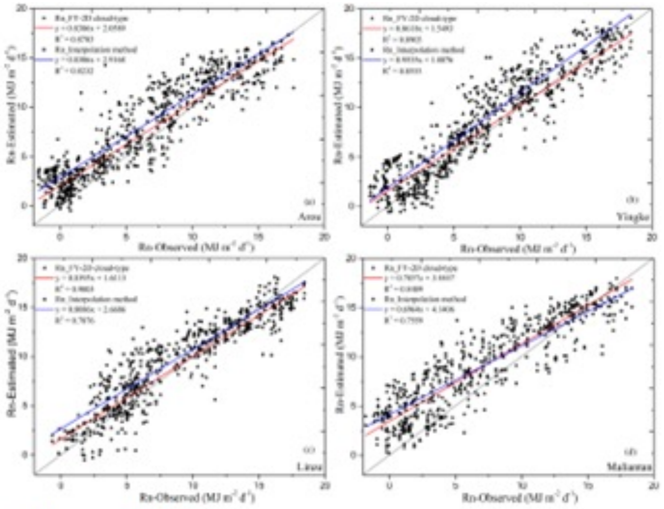

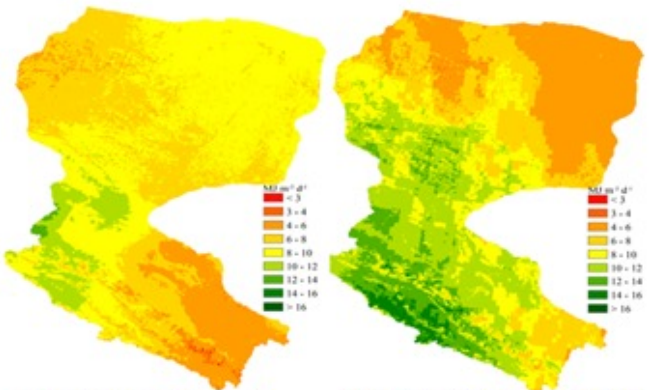

Wu B F, et al. 2017. An Improved Approach for Estimating Daily Net Radiation over the Heihe River Basin. Sensors, 17, 86.
Wu B F, et al. 2016. A Method to Estimate Sunshine Duration Using Cloud Classification Data from a Geostationary Meteorological Satellite (FY-2D) over the Heihe River Basin. Sensors, 16, 1859

Atmospheric Boundary Layer height (ABL)

- ***The characteristic of the atmospheric boundary layer height is a key factor in the ET process. Other remote sensing ET models use a fixed boundary layer height value, which seriously affects the interannual stability of evapotranspiration.***
  - *Atmospheric boundary layer height* models *are proposed to accurately describe the spatial heterogeneity of boundary layer parameters based on atmospheric profile data*
  - *With this method, we can reduce the sensitivity of ETWatch to the thermal character of ground, then improve the accuracy of ET model*

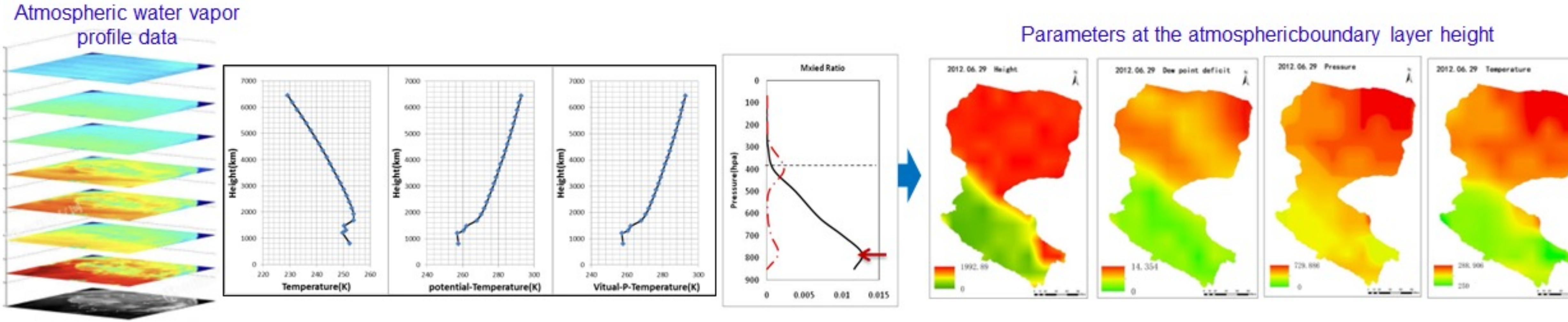

Xueliang Feng, Bingfang Wu, Nana Yan, Weiwei Zhu. Method to derived mixed boundary layer height from MODIS atmospheric profile data product at Heihe river basin. Atmosphere 2015, 6, 1346-1361; doi:10.3390/atmos609134

Vapor pressure deficit (VPD)

- ***Vapor pressure deficit models are proposed to accurately describe the spatial heterogeneity of Vapor pressure deficit based on atmospheric profile data and atmospheric precipitable data products***

Atmospheric water vapor profile data

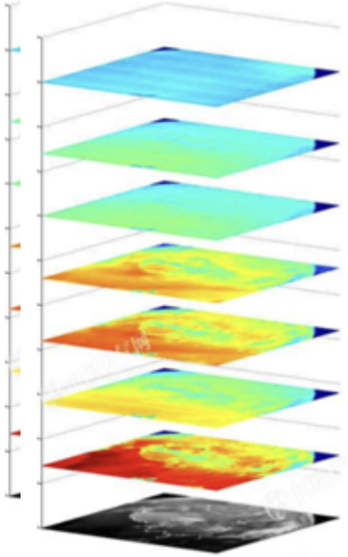

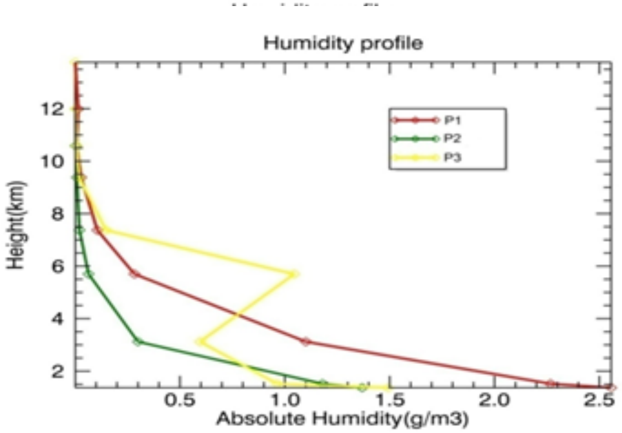

P1: Standard atmospheric profiles;
$R=1.05, A_1=0.92, A_2=0.46$;
P2: Near-surface dry atmospheric profiles at wet high-altitude;
$R=0.53, A_1=0.94, A_2=0.36$;
P3: Near-surface wet atmospheric profiles at dry high-altitude;
$R=3.53, A_1=0.8, A_2=0.85$.
A_1, A_2 reflects the status of humidity profiles

- ***Instantaneous near-surface vapor pressure:***

$$R = \frac{(RH_{700} + RH_{600} + RH_{500})/3}{RH_{850}}$$

$$A_1 = 0.91 + 0.1 * \left(1 - \frac{(RH_{500} + RH_{400})/2}{(RH_{700} + RH_{600} + RH_{500})/3}\right)$$

$$A_2 = 0.51 + 0.128 \ln(R)$$

$$a = TPW \cdot A_1 \cdot 10000 /(H_{500\ hPa} - H)/A_2$$

$$e_a = 0.125 \cdot a \cdot (1 + T_a/273.15)$$

- *Instantaneous near-surface air temperatures and VPD calculation:*

$$T_s - T_a = k_0 + k_1 \cdot NDVI + k_2 \cdot W$$

$$VPD = e^*(T_a) - e_a$$

Hongmei Zhong, Bingfang Wu, et al. An improved satellite-based apporach for estimating vapor pressure deficit from MODIS data. Journal of Geophysical Research: Atmospheres. 119, 12256-12271

Estimation and Validation of VPD

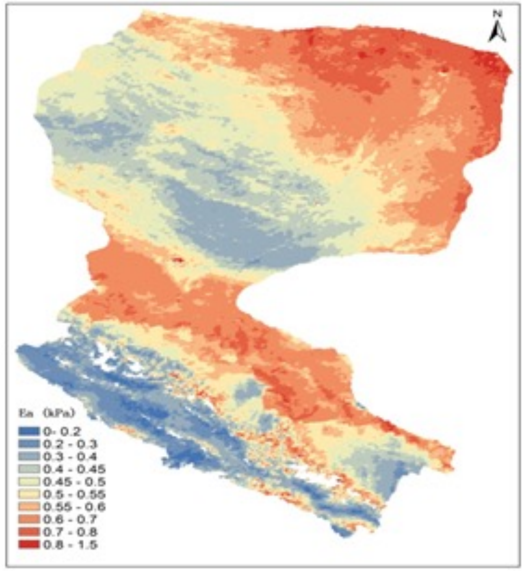

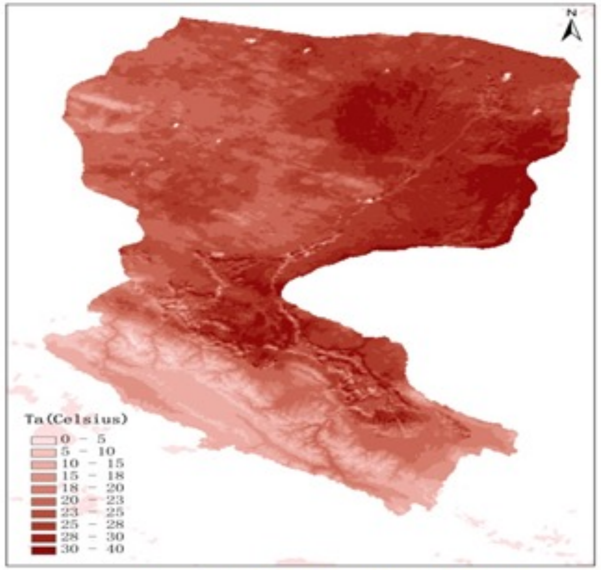

Near-surface air temperature

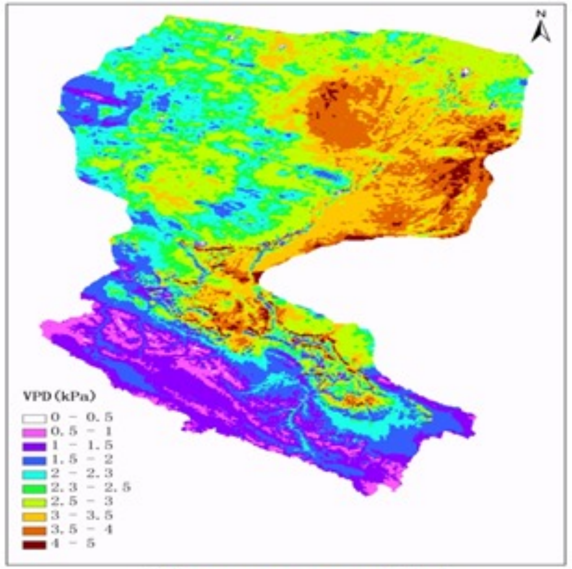

Vapor pressure deficit

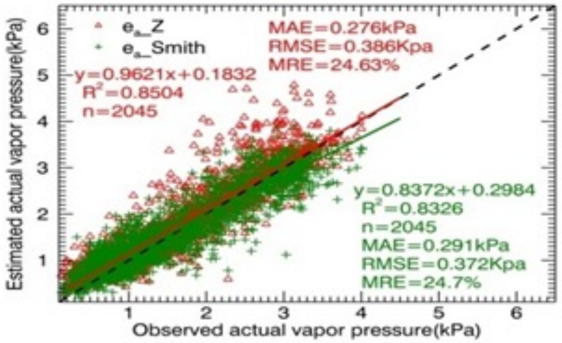

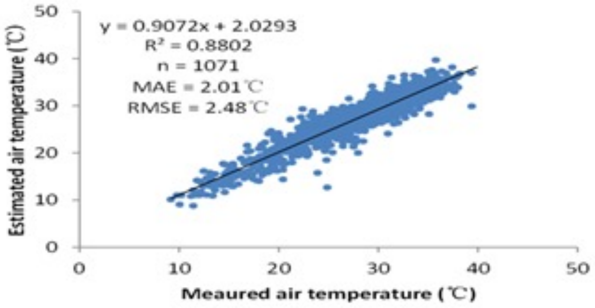

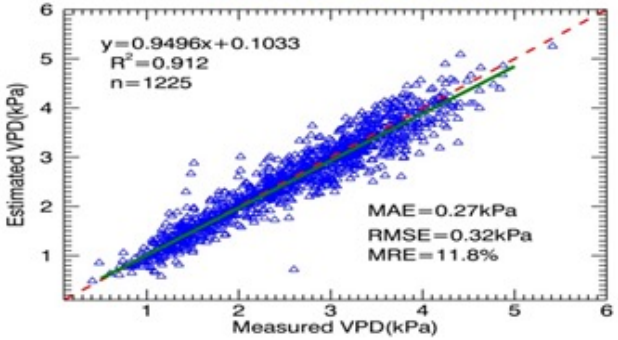

Hongmei Zhong, Bingfang Wu, et al. An improved satellite-based apporach for estimating vapor pressure deficit from MODIS data. Journal of Geophysical Research: Atmospheres. 119, 12256-12271

ETWatch System-ETWatch Standalone

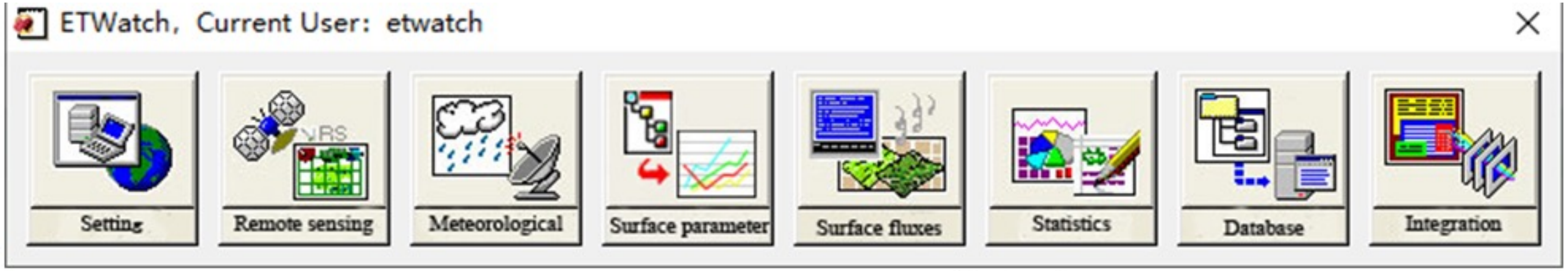

Data flow

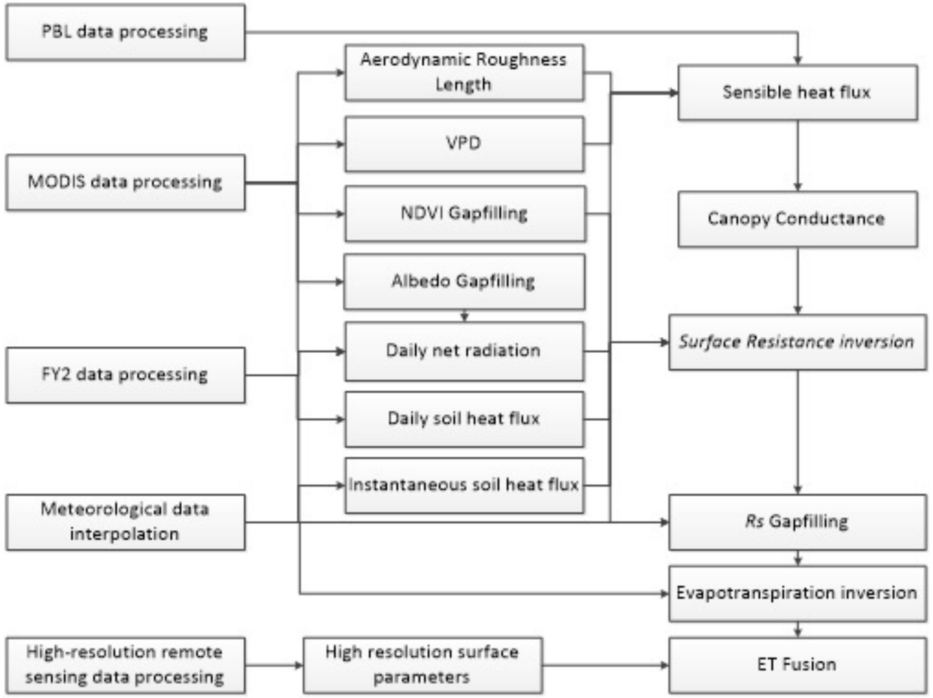

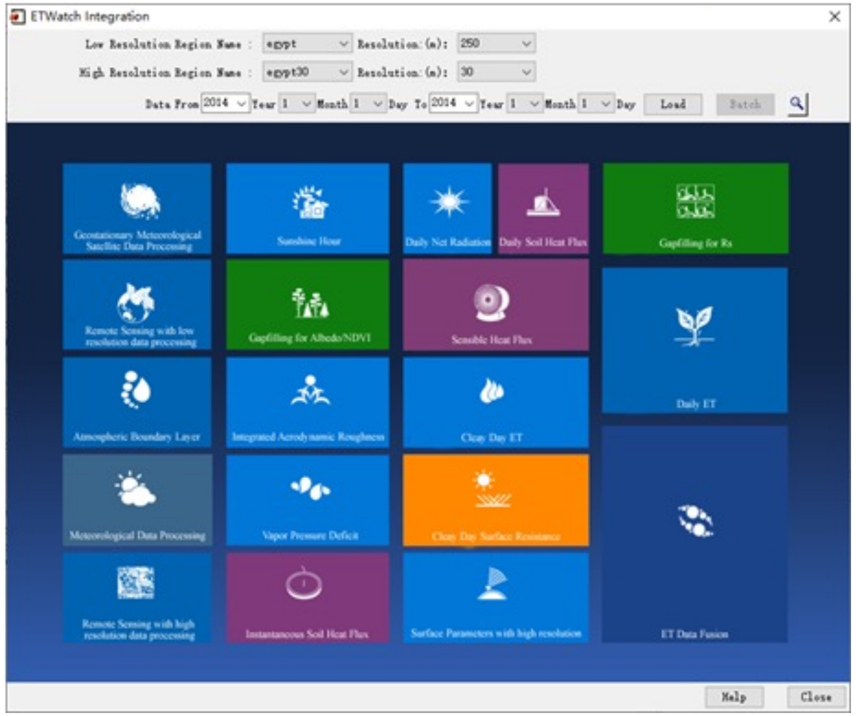

ETWatch System-ETWatch Standalone

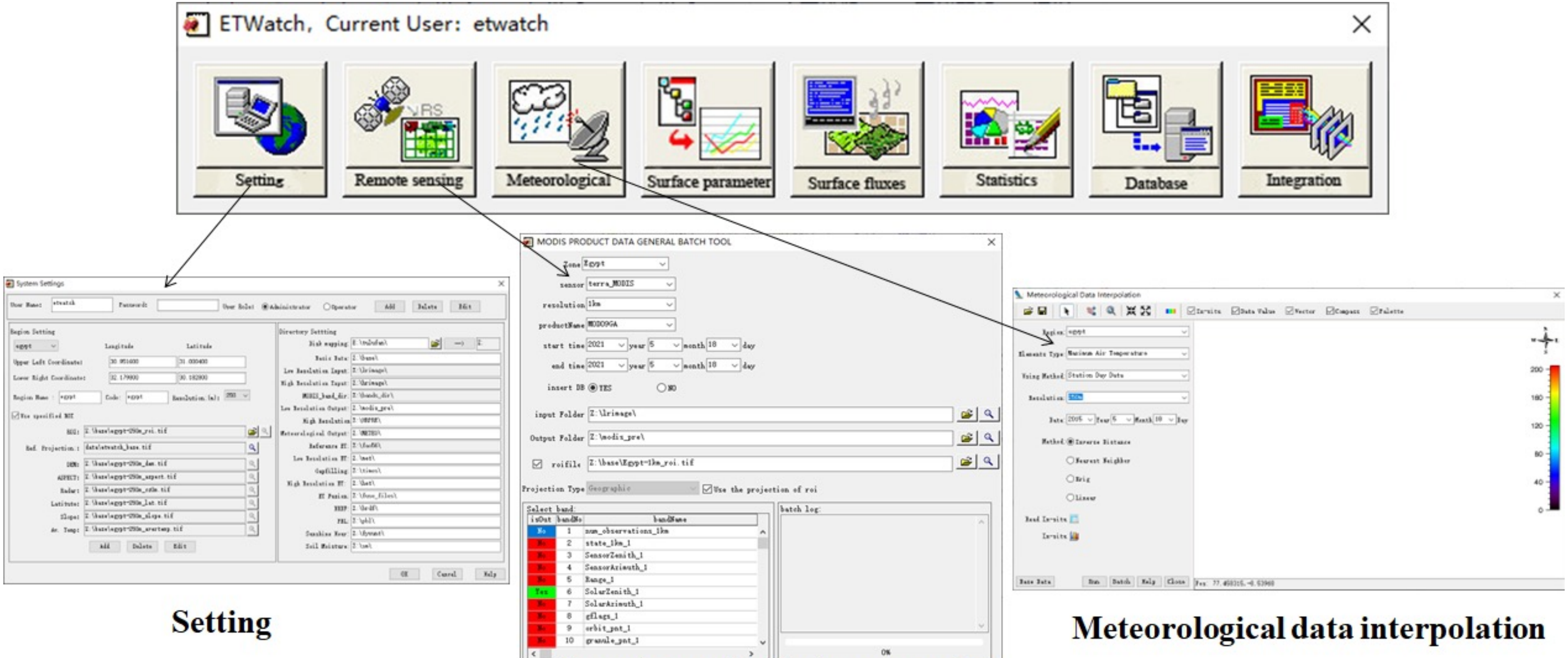

Setting

Remote sensing data processing

Meteorological data interpolation

ETWatch System-ETWatch Standalone

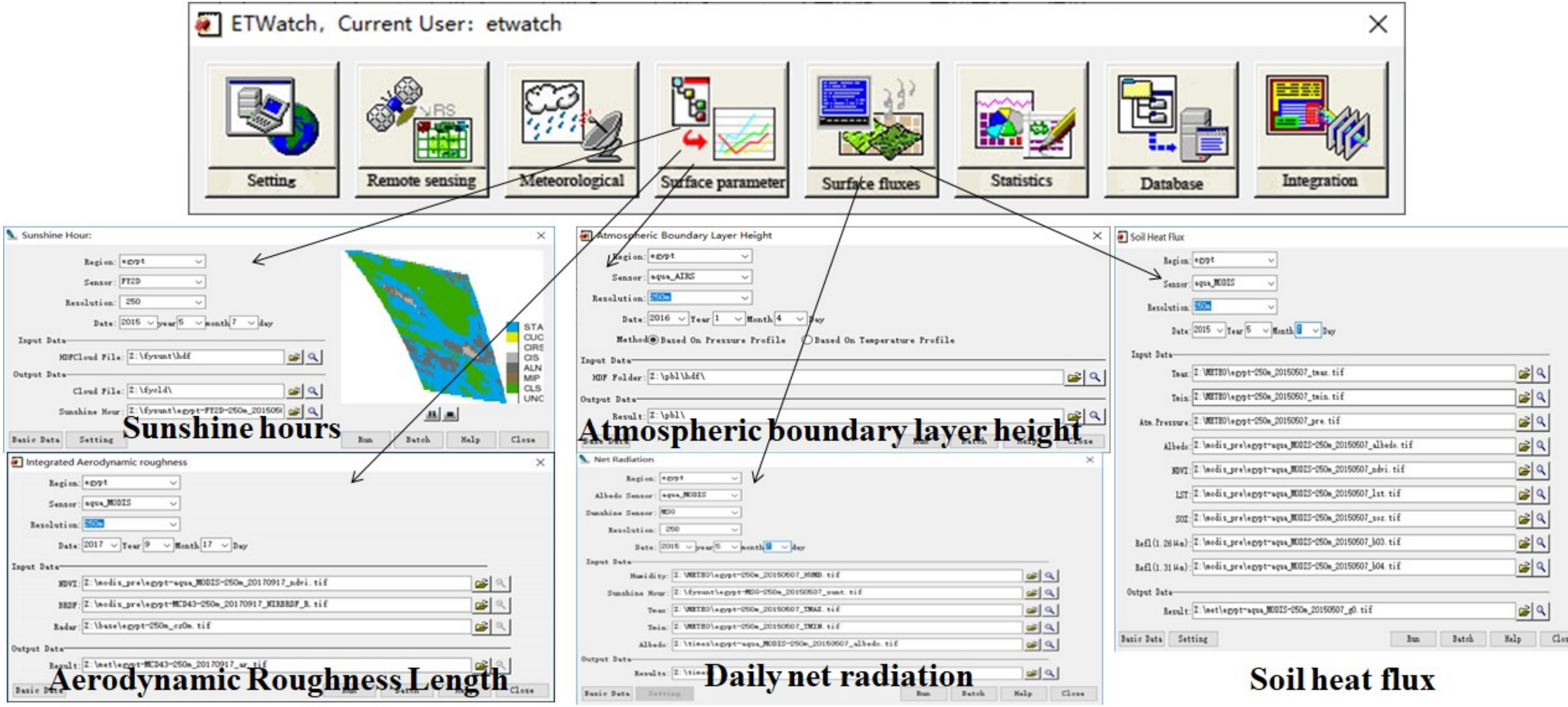

ETWatch System-ETWatch Standalone

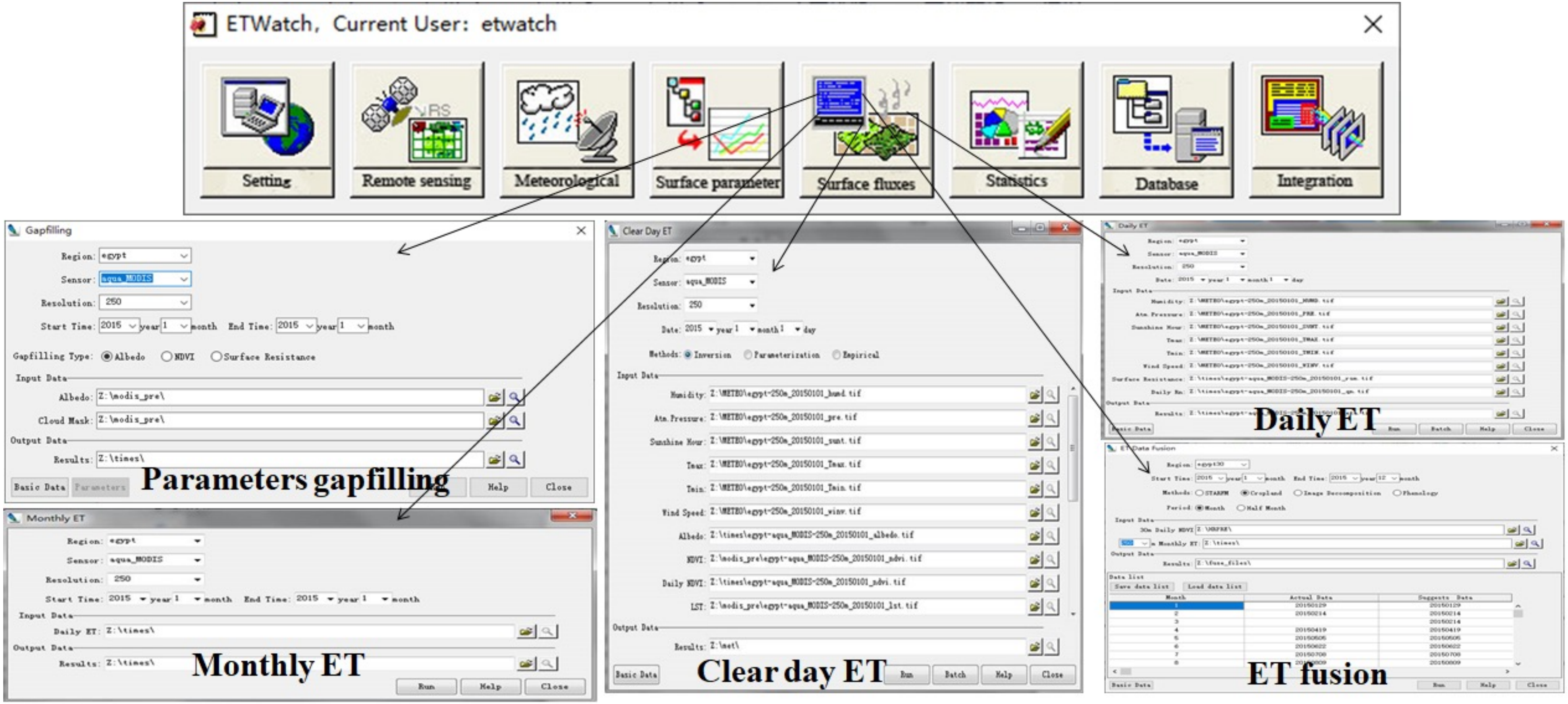

ETWatch System-ETWatch Standalone

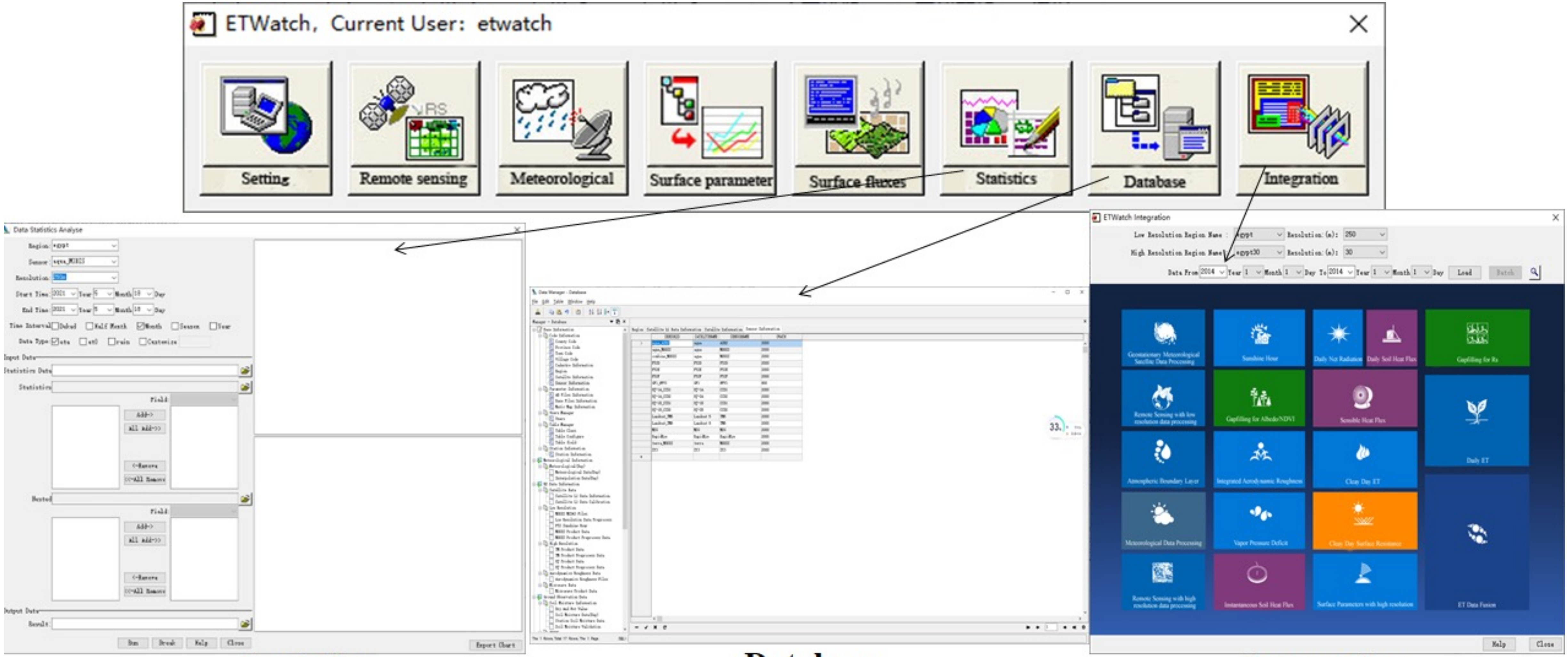

Statistics Database Integration

ETWatch System-ETWatch Cloud

Using analysis

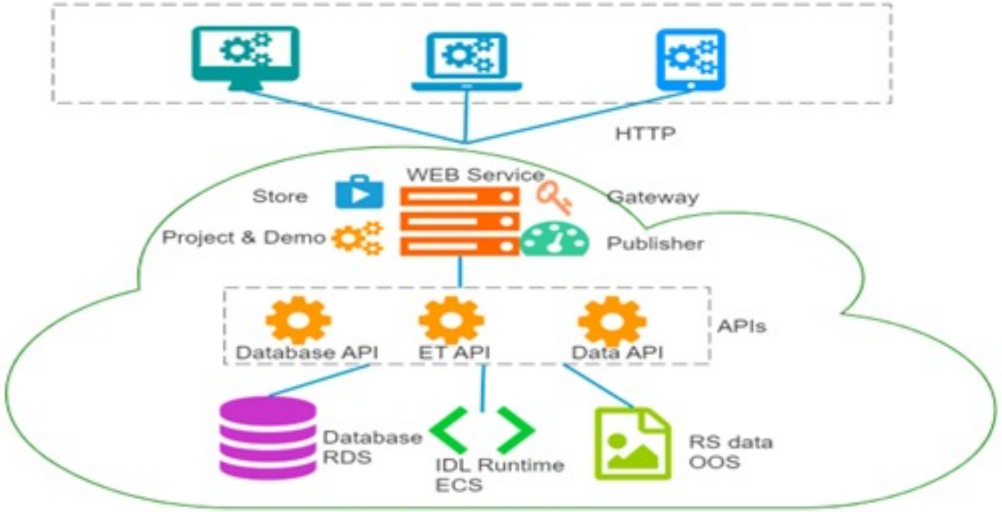

Framework

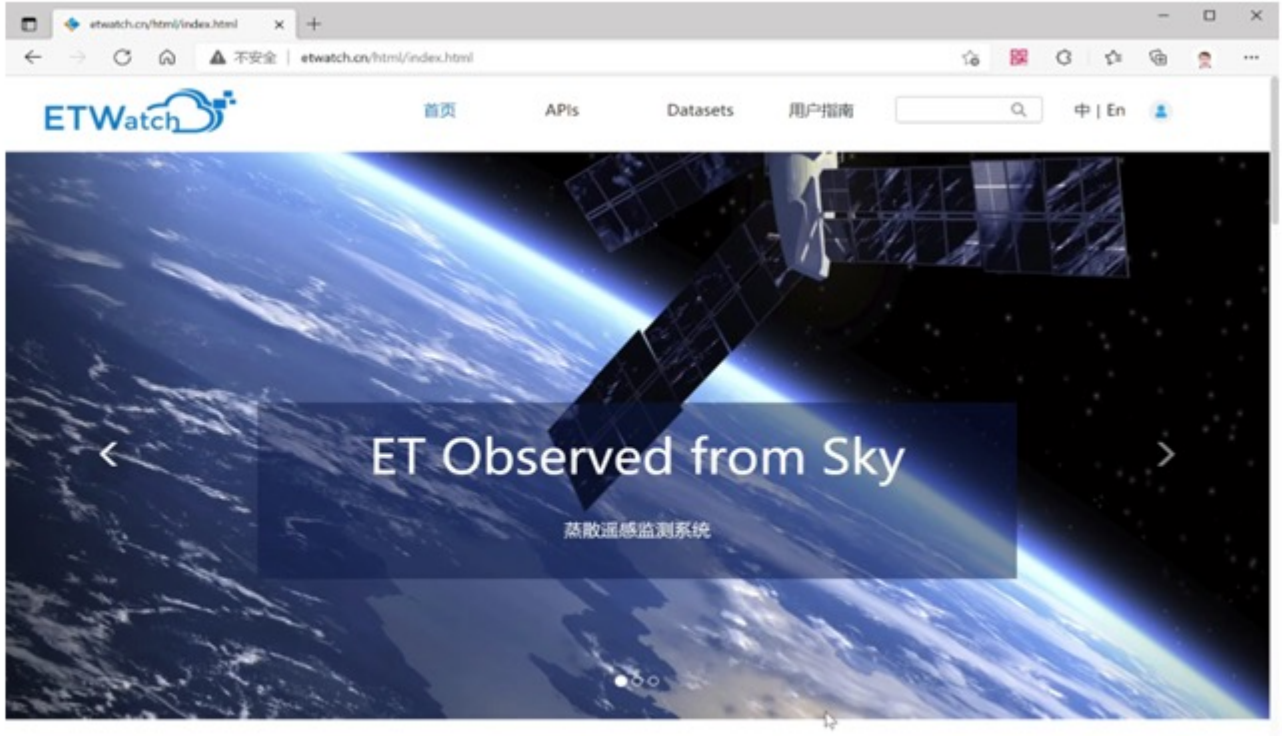

APIs List

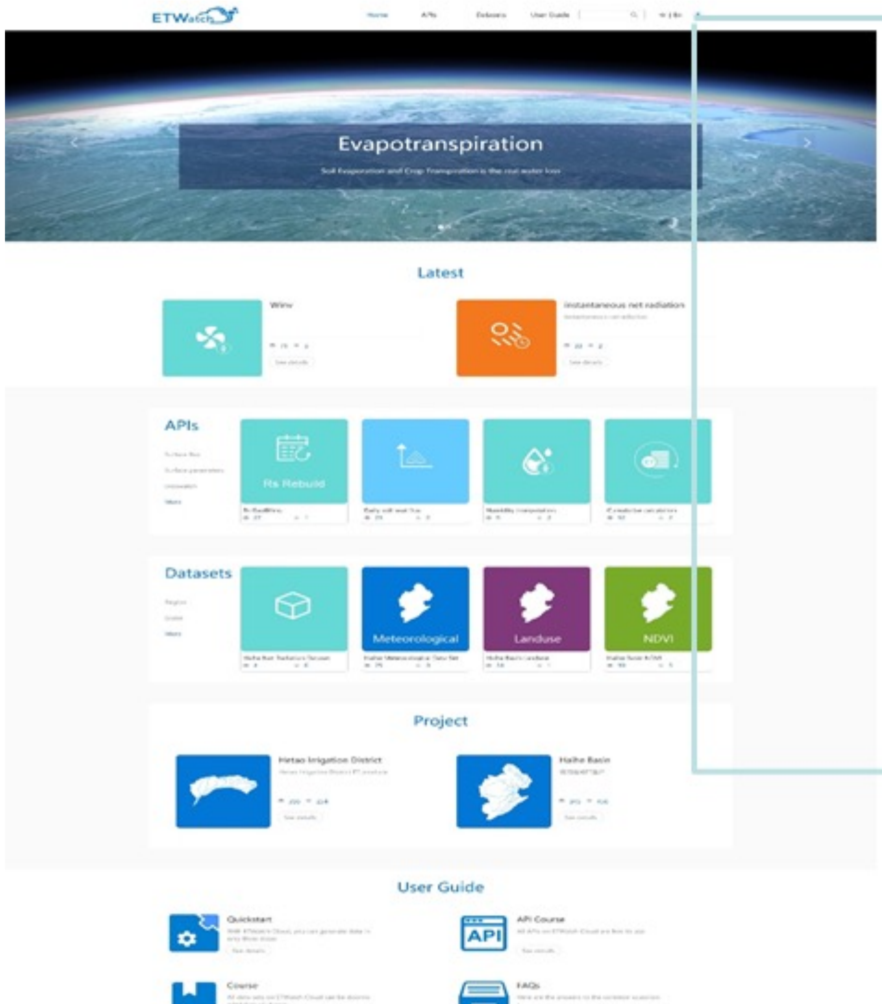

Homepage

Register

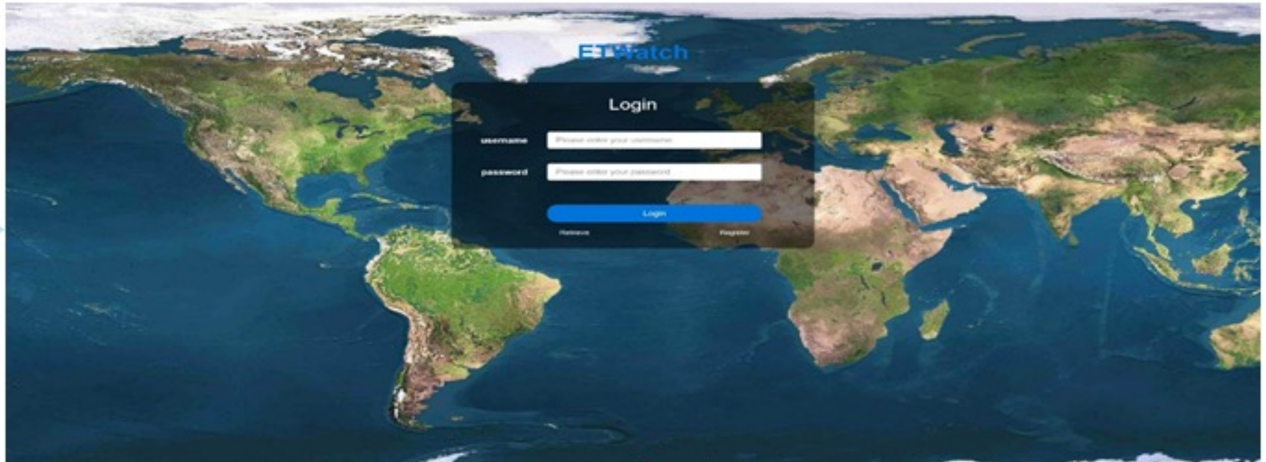

Login

ETWatch System-ETWatch Cloud

Call APIs and MyCollection

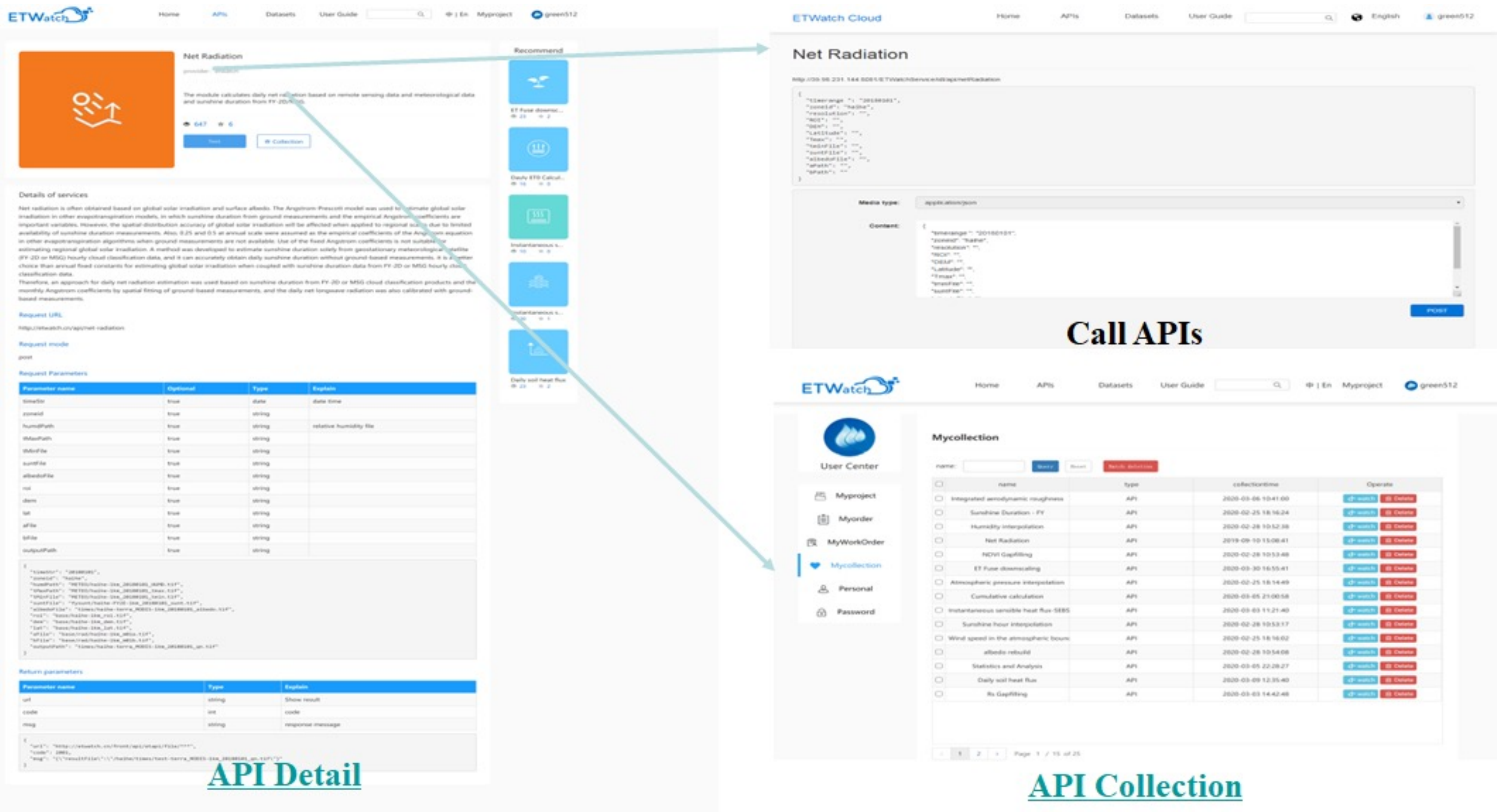

API Detail

API Collection

ETWatch System-ETWatch Cloud

Setting own project

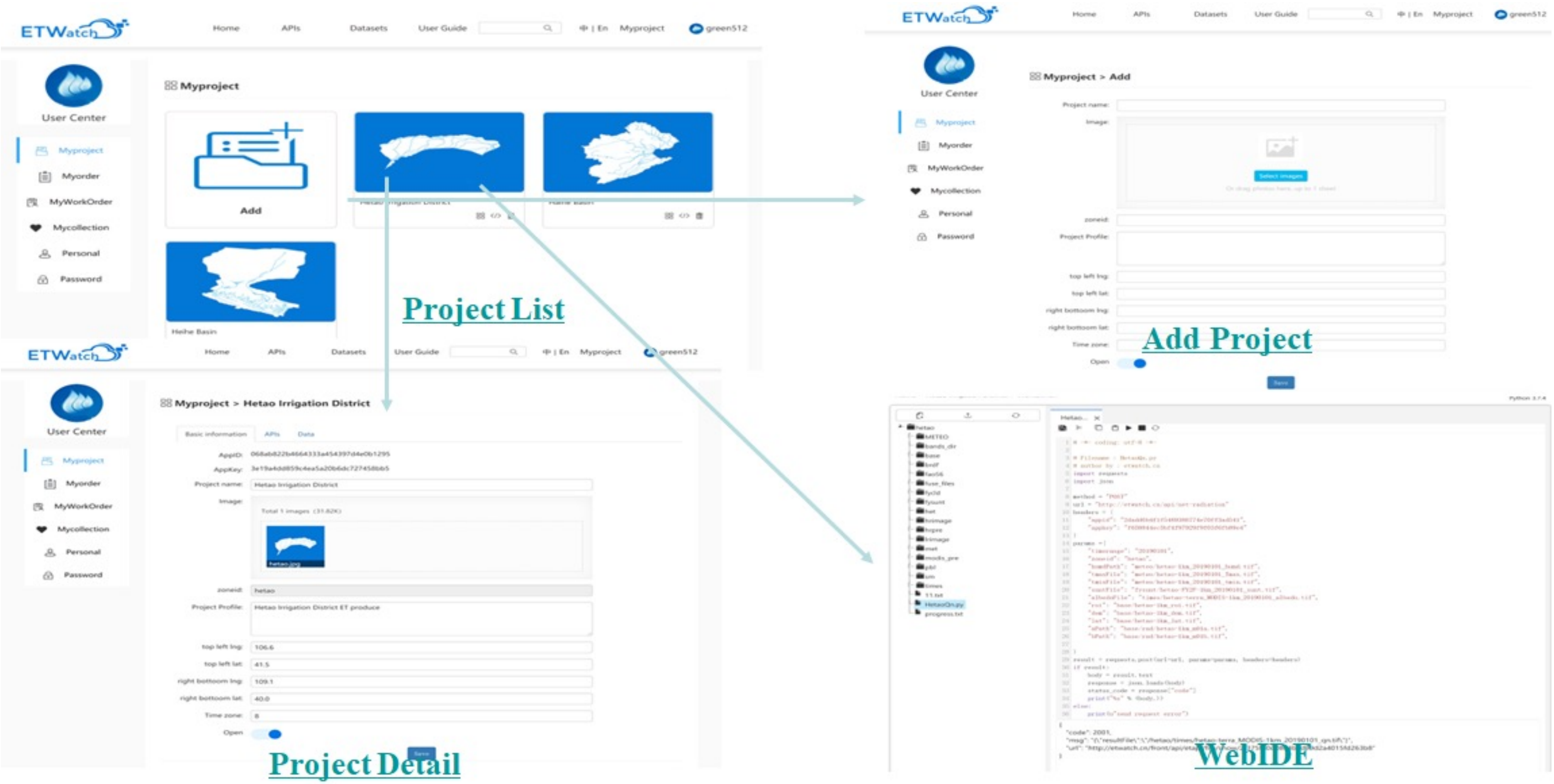

ETWatch System-ETWatch Cloud

API Add and Run

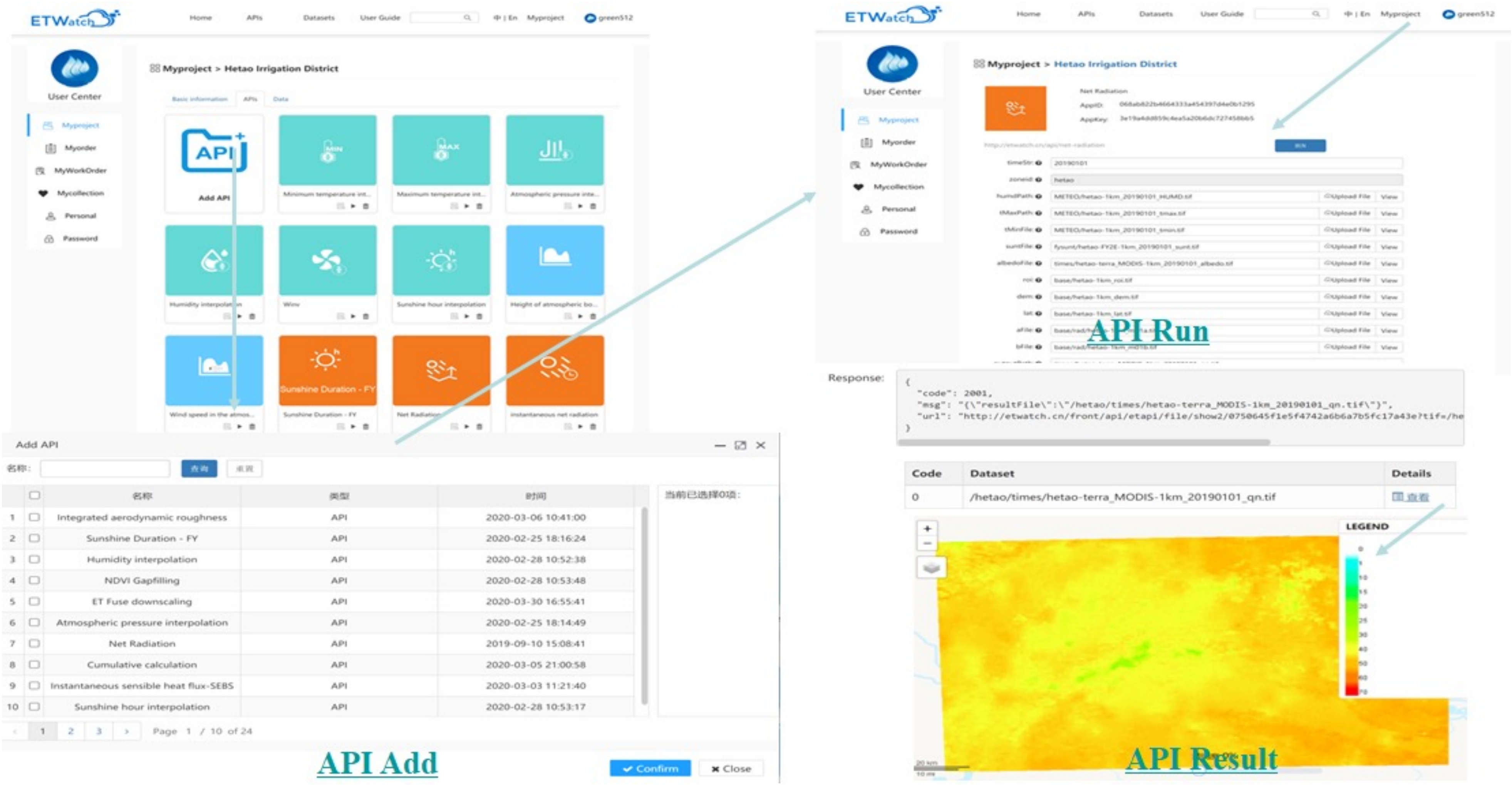

ETWatch Features

- ***ET resolution is from 5m to 1km in global scale or regional scale***
- ***Multi-party independent validation: annual accuracy of 97%, daily accuracy of 90-93%***
- ***Model***
  - *Quantifying fluxes between land surface, soil, vegetation, and the atmospheric boundary layer using multi-source satellite data*
  - *Solve the problem of large uncertainty and poor regional applicability of remote sensing ET model on the complex underlying surface*
  - *Reduces the multicollinearity problem between multiple key variables in ET models*
  - *Solve the mismatch problem between the spatial and temporal resolution of remote sensing data and the time-continuous process of evapotranspiration, and obtain multi-scale remote sensing ET data with high spatiotemporal resolution*
  - *ET downscaling and field scale ET allocation at agricultural parcel and hydrological element for high resolution with support of multi-temporal optical satellite data*

Key Results

- ***ET data in North China region and some European countries were produced using ETWatch model***
  - Field data from 2 field stations (Guantao, Huailai) in Hebei provice in China was used for accuracy validation
  - RMSE is about 1 mm/day, the R^2 is about 0.8. The result of accuracy validation shows that the ETWatch model can well estimate ET. The data can be used for spatio-temporal characteristics analysis.

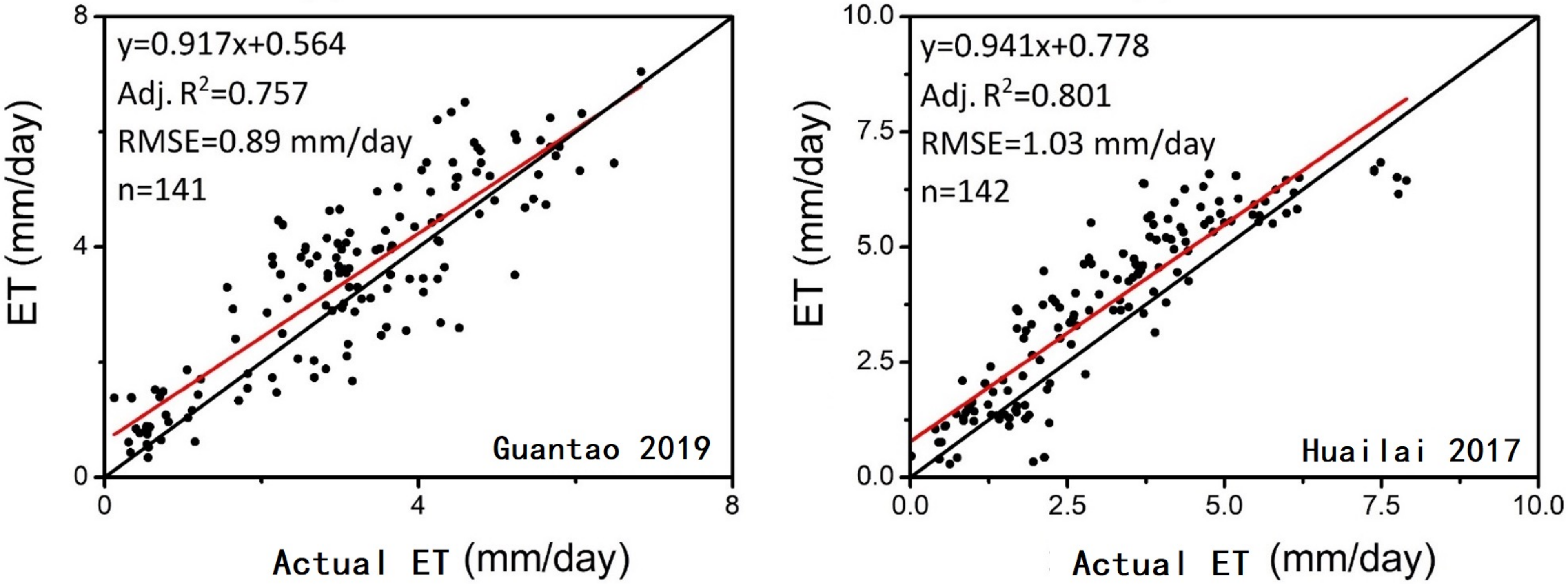

Key Results

- ***Spatio-temporal characteristics analysis of ET in China and Europe***
  - The North China region has a high vegetation cover, vegetation transpiration resulted in low ET in this area.
  - Significant difference was exisited in East and West of North China region
  - Average ET in Belgium is 12.75 mm, and the ET in south of Belgium is lower than north

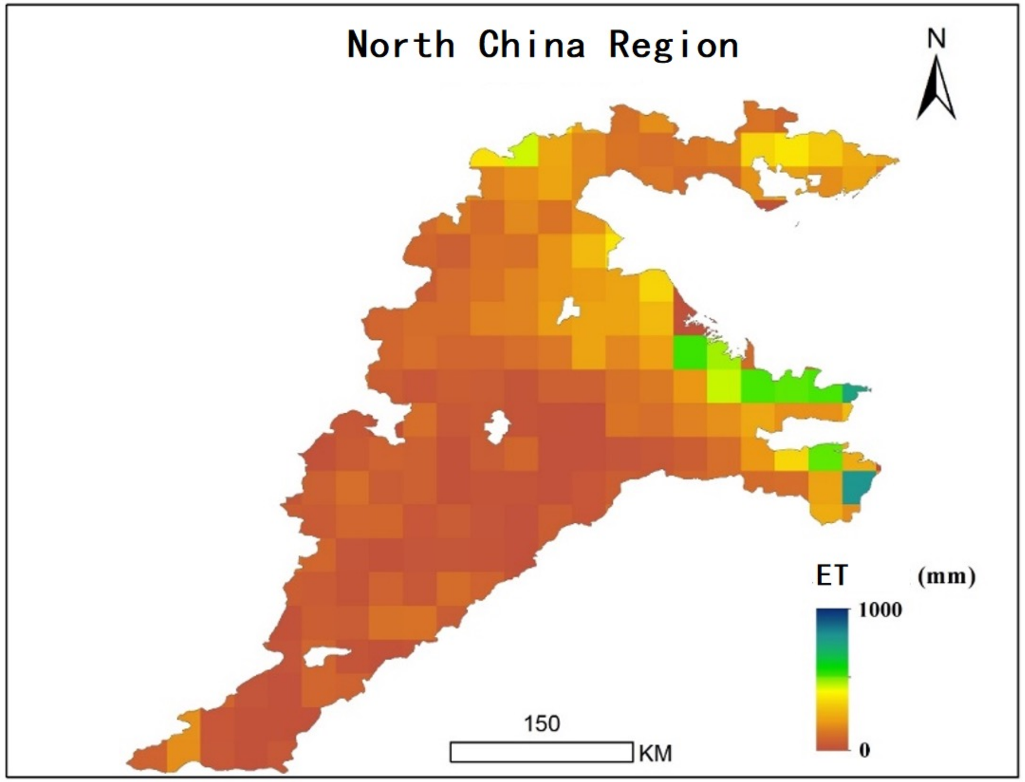

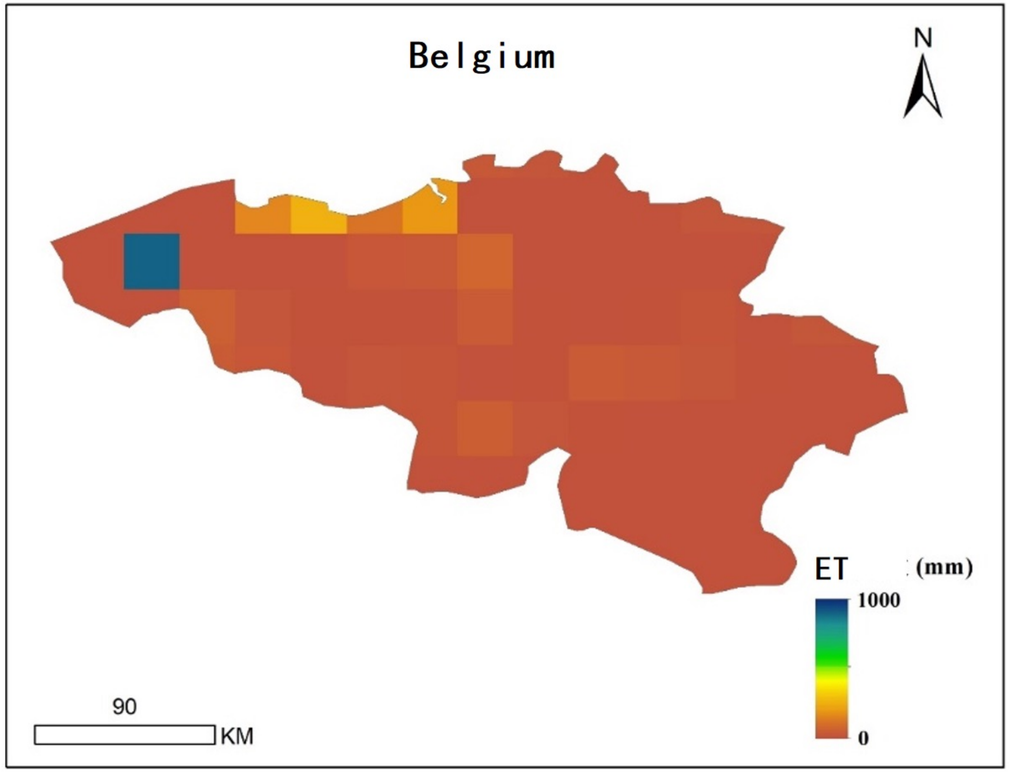

Key Results

■ ***Spatio-temporal characteristics analysis of ET in China and Europe***

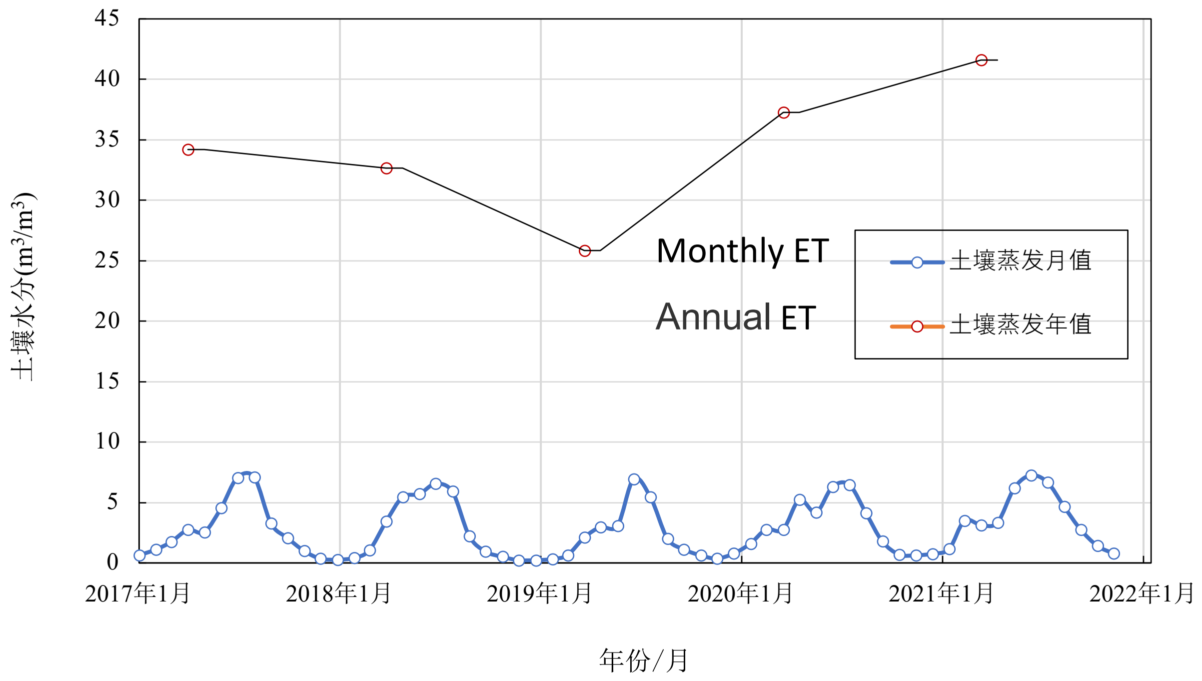

North China

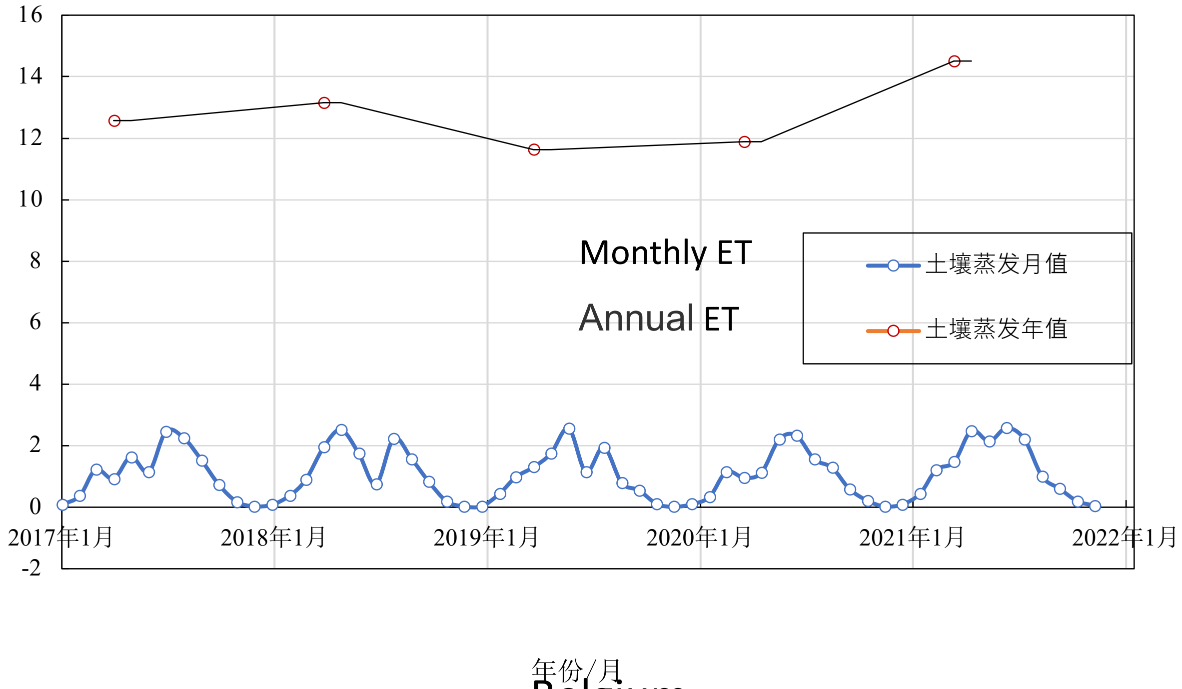

Belgium

Key Results

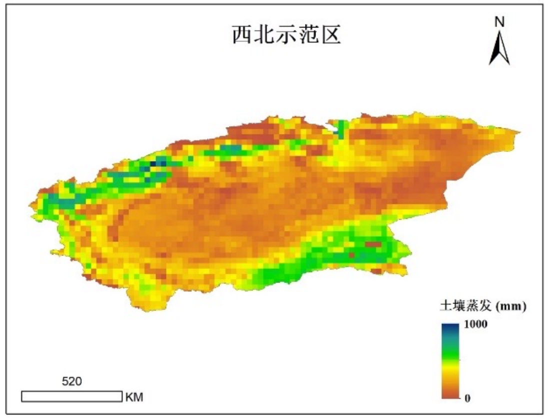

NorthEast China

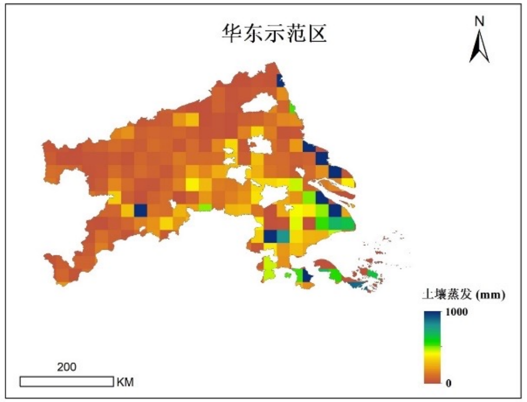

East China

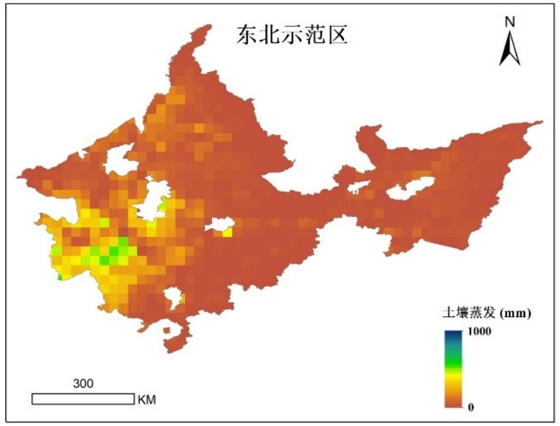

NorthEast China

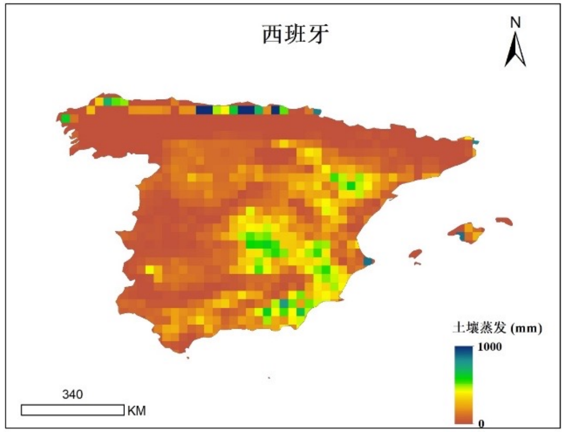

Spain

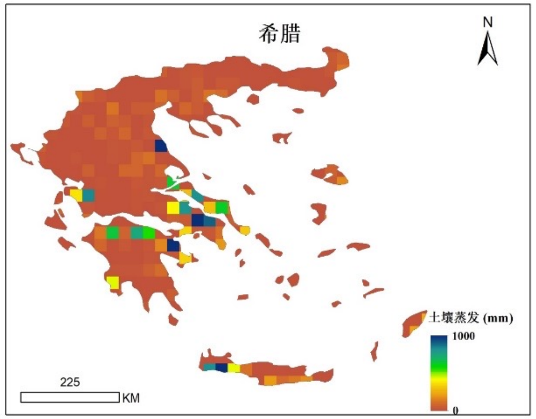

Greece

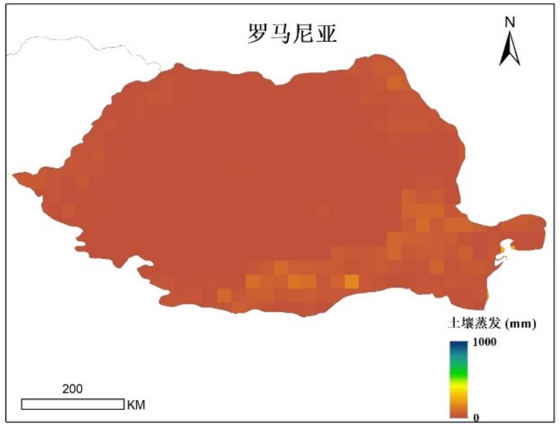

Romania

Young scientists contributions in Dragon 5

Name	Institution	Poster title	Contribution including period of research
Ilina Kamenova	Space Research and Technology Institute, Bulgarian Academy of Sciences	Evapotranspiration estimation using Sen-ET SNAP Plugin for study area in Bulgaria （ID:249）	ET in cropland in Bulgaria

Thanks for your attention

zhuliang@aircas.ac.cn